STP-PT-043

ASME FLAWED CYLINDER TESTING

ASME STANDARDS TECHNOLOGY, LLC

STP-PT-043

ASME FLAWED CYLINDER TESTING

ASME STANDARDS TECHNOLOGY, LLC

Date of Issuance: December 17, 2010

This report was prepared as an account of work sponsored by ASME Pressure Technologies Codes and Standards and the ASME Standards Technology, LLC (ASME ST-LLC).

ASME Standards Technology, LLC
Three Park Avenue, New York, NY 10016-5990
ISBN No. 978-0-7918-3353-7

TABLE OF CONTENTS

Foreword iv
Abstract v
1 INTRODUCTION 7
2 PRESSURE VESSEL CONFIGURATION 8
3 TEST PLAN 9
4 FLAWS 10
5 FATIGUE TEST 13
6 BURST TESTING 15
7 RESULTS AND DISCUSSION 16
8 SUMMARY AND CONCLUSIONS 19
Appendix A 20
Appendix B 33
Appendix C 46
Acknowledgments 72

LIST OF TABLES

Table 1 - Randomly Assigned Tank Numbers, Flaw Depths and Number of Cycles 9
Table 2 - Test Tank Flaw Depths Using the Nominal Structural Composite Thickness of 11.4mm (0.449 inches) 10
Table 3 - Pressure Cycling Tests Results 13
Table 4 - Summary of Burst Data 15
Table 5 - Comparison of Burst Data 17

LIST OF FIGURES

Figure 1 - Composite Pressure Vessel, P/N 240075-023 8
Figure 2 - Location of Flaws on the Tanks 11
Figure 3 - Locations of Longitudinal and Transverse Flaws 11
Figure 4 - Cross-Sectional View of Flaw 12
Figure 5 - Record of Flaw Depths, in Inches, after Machining 12
Figure 6 - Longitudinal Flaw in Tank 3B Before Cycling 14
Figure 7 - Longitudinal Flaw in Tank 3B after 20,000 Cycles 14
Figure 8 - Burst Pressure Versus Depth of Flaw and Cycling 18
Figure 9 - Burst Pressure Versus Cycling and Depth of Flaw 18

FOREWORD

The ASME BPV Project Team on Hydrogen Tanks, in conjunction with other ASME Codes and Standards groups, is developing Code Cases and revisions to the Boiler & Pressure Vessel Code, including such to address the design of composite pressure vessels. The project team had an interest in further understanding the effect of cuts to the surface of composite tanks, and how the burst pressure would be affected during the lifetime of the pressure vessel.

A test program was initiated to provide data on initial burst pressure, and burst pressure after pressure cycling, of composite cylinders with cuts of different depths. These results were considered during the development and approval of the ASME Code Cases and Code revisions.

Established in 1880, the American Society of Mechanical Engineers (ASME) is a professional not-for-profit organization with more than 127,000 members promoting the art, science and practice of mechanical and multidisciplinary engineering and allied sciences. ASME develops codes and standards that enhance public safety, and provides lifelong learning and technical exchange opportunities benefiting the engineering and technology community. Visit www.asme.org for more information.

The ASME Standards Technology, LLC (ASME ST-LLC) is a not-for-profit Limited Liability Company, with ASME as the sole member, formed in 2004 to carry out work related to newly commercialized technology. The ASME ST-LLC mission includes meeting the needs of industry and government by providing new standards-related products and services, which advance the application of emerging and newly commercialized science and technology and providing the research and technology development needed to establish and maintain the technical relevance of codes and standards. Visit www.stllc.asme.org for more information.

ABSTRACT

The effect of flaws with and without cyclic loading was investigated on a composite overwrapped pressure vessel with a non-load sharing polymer liner. Flaws were machined in the structure to four depths and then were cycled for 0, 10,000 and 20,000 cycles. Finally, the cylinders were hydrostatically burst. These data were compared to a reference burst value of a cylinder without flaws or cycles. The cylinder was 406 mm (16 in.) in diameter by 1020 mm (40 in.) long with a service pressure rating of 24.8 MPa (3600 psi).

The lowest burst-to-operating pressure ratio was 2.13, which occurred with the flaws cut 40% into the structure and no cycles. Even with the deepest flaw and cycling, the resulting burst pressure margin would allow safe operation of the pressure vessel over a period of time. The lack of significant additional strength loss with cycling gives a degree of confidence that even if flaws are not found immediately, the risk of a failure due to the flaw is low.

INTENTIONALLY LEFT BLANK

1 INTRODUCTION

The ASME BPV Project Team on Hydrogen Tanks, in conjunction with other ASME Codes and Standards groups, is developing Code Cases and revisions to the Boiler & Pressure Vessel Code, including such to address the design of composite pressure vessels. The Project Team had an interest in further understanding the effect of cuts to the surface of composite tanks, and how the burst pressure would be affected during the lifetime of the pressure vessel.

A test program was initiated to provide data on initial burst pressure, and burst pressure after pressure cycling, of composite cylinders with cuts of different depth. These results were considered during the development and approval of the ASME Code Cases and Code revisions.

The effect of flaws with and without cyclic loading was investigated on a composite overwrapped pressure vessel with a non-load sharing polymer liner. Flaws were machined in the structure to four depths and then were cycled for 0, 10,000 and 20,000 cycles. Finally the cylinders were hydrostatically burst. These data were compared to a reference burst value of a cylinder without flaws or cycles. The cylinder was 406 mm (16 in.) in diameter by 1020 mm (40 in.) long with a service pressure rating of 24.8 MPa (3600 psi).

The lowest burst-to-operating pressure ratio was 2.13, which occurred with the flaws cut 40% into the structure and no cycles. Even with the deepest flaw and cycling, the resulting burst pressure margin would allow safe operation of the pressure vessel over a period of time. The lack of significant additional strength loss with cycling gives a degree of confidence that even if flaws are not found immediately, the risk of a failure due to the flaw is low.

2 PRESSURE VESSEL CONFIGURATION

The pressure vessels tested were constructed of fiber reinforced resin wound over a non-metallic liner. The liner material was high-density polyethylene (HDPE). Bosses, or nozzles, were made of 6061-T6 aluminum that were molded into the ends of the liner. These bosses are the interface for filling and pressurizing the vessel. The primary reinforcement was T-700 carbon fiber. Glass fiber was co-mingled with the carbon in the structural layers. There was also a sacrificial wrapping of glass fiber on the outside of the vessel. The resin matrix was epoxy.

The pressure vessels were 406 mm (16 in.) in diameter, and 1020 mm (40 in.) long. One of the cylinders is shown in Figure 1. It was designed for a nominal service pressure of 24.8 MPa (3600 psi) and a minimum burst pressure of 64.8 MPa (9400 psi) when accounting for the glass and sacrificial overwrap. The structural composite was 11.4 mm (0.45 in.) thick and the sacrificial outer glass reinforced layer was 2.0 mm (0.08 in.) thick.

Figure 1 - Composite Pressure Vessel, P/N 240075-023

3 TEST PLAN

Fifteen composite overwrapped pressure vessels P/N 240075-023 were manufactured in April 2009. The S/N's were 1007-001 through 1007-015. Inspection of the manufacturing data revealed that S/N 1007-007 was slightly heavier than the rest of the PV's in this lot; therefore, this tank was tagged as one of the two "spares" for testing. Flaws that range from 1.27 mm (0.050 in.) (approximately 10%) up to 40% through the composite were machined into 12 tanks. One additional tank without the machined flaws was burst as a control. Tanks were to be burst after 0, 5000 or 10,000 cycles. However, since cycling the tanks with the flaws to 10,000 cycles did not significantly decrease the burst pressure, it was decided to cycle the remaining set to 20,000 cycles rather than the originally planned 5000 cycles. The use of a non-load sharing HDPE liner in these pressure vessels allows higher number of pressure cycles without the risk of leaking due to liner fatigue. S/N's were randomly assigned to each test and are listed in **Table 1**.

Table 1 - Randomly Assigned Tank Numbers, Flaw Depths and Number of Cycles

Test Tank	SN [1]	Flaw Depth (% of structural thickness)	Cycles
5	1007-014	none	0
4A	1007-005	1.27 mm (0.050") 10%	0
1A	1007-002	20%	0
2A	1007-009	30%	0
3A	1007-011	40%	0
4C	1007-010	1.27 mm (0.050") 10%	10k
1C	1007-001	20%	10k
2C	1007-015	30%	10k
3C	1007-013	40%	10k
4B	1007-006	1.27 mm (0.050") 10%	20k
1B	1007-003	20%	20k
2B	1007-004	30%	20k
3B	1007-012	40%	20k

[1] Chosen at random

1007-008 Damaged during flaw procedure

1007-007 Slightly heavy from manufacturing process, used as flaw practice tank

4 FLAWS

For the tanks with flaws, two flaws were machined into the composite laminate. Since these composite pressure vessels contained a sacrificial glass overwrap, the first step was to remove a portion of the glass to expose the structural composite layer. The removal of this layer was performed on all of the tanks regardless of whether a flaw was to be machined into the structural layer. The depths of the flaws are listed in Table 1.

The flaw requirements are as follows.

Flaws were made using a 1 mm diameter ball-end cutter to a depth listed in **Table 2**. The length of each flaw was 57.0 +/- 0.13 mm (2.245 +/- 0.005 in.) as measured from the center of the cutter. This flaw length was five times the structural laminate thickness of 11.4 mm (0.449 in.) based on the flaw test requirement of ISO 11119-3. The longitudinal flaw was cut at the mid-length of the pressure vessel. The transverse flaw was cut at the mid-length of the pressure vessel approximately 120° from the longitudinal flaw. Schematic drawings of these locations are shown in Figure 2 through Figure 4. Dimensions were measured and recorded for each flaw and are shown in Figure 5. Each flaw was photo-documented and is shown in Appendix A.

The structural laminate was a combination of approximately 43% helical reinforcement and 57% circumferential reinforcement patterns. The reduction of these reinforcements due to the flaws are also listed in Table 2.

Table 2 - Test Tank Flaw Depths Using the Nominal Structural Composite Thickness of 11.4 mm (0.449 in.)

Test Tank	SN [(I)]	Longitudinal Flaw Depth +/- 0.13 mm (0.005") mm (inches)	Transverse Flaw Depth +/- 0.13 mm (0.005") mm (inches)	Reduction in Helical Reinforcement	Reduction in Circumferential Reinforcement
IA	1007-002	2.3 (0.090)	2.3 (0.090)		
IB	1007-003	2.3 (0.090)	2.3 (0.090)		
IC	1007-001	2.3 (0.090)	2.3 (0.090)	17 %	22%
2A	1007-009	3.43 (0.135)	3.43 (0.135)		
2B	1007-004	3.43 (0.135)	3.43 (0.135)		
2C	1007-015	3.43 (0.135)	3.43 (0.135)	33%	28%
3A	1007-011	4.57 (0.180)	4.57 (0.180)		
3B	1007-012	4.57 (0.180)	4.57 (0.180)		
3C	1007-013	4.57 (0.180)	4.57 (0.180)	45%	38%
4A	1007-005	1.27 (0.050)	1.27 (0.050)		
4B	1007-006	1.27 (0.050)	1.27 (0.050)		
4C	1007-010	1.27 (0.050)	1.27 (0.050)	8%	13%
5	1007-014	glass removal only	glass removal only	0	0

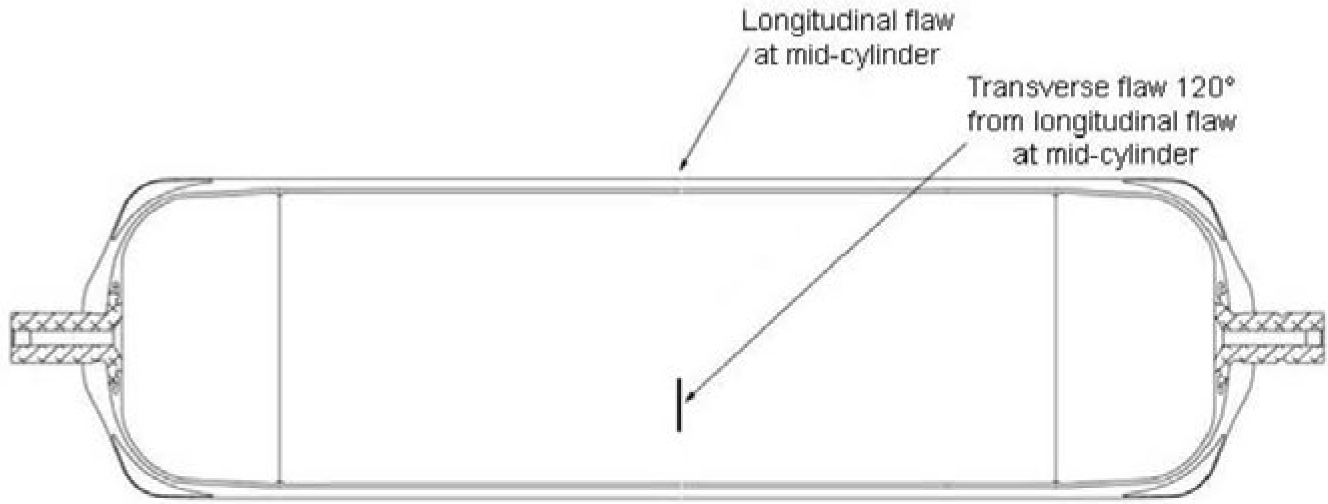

Figure 2 - Location of Flaws on the Tanks

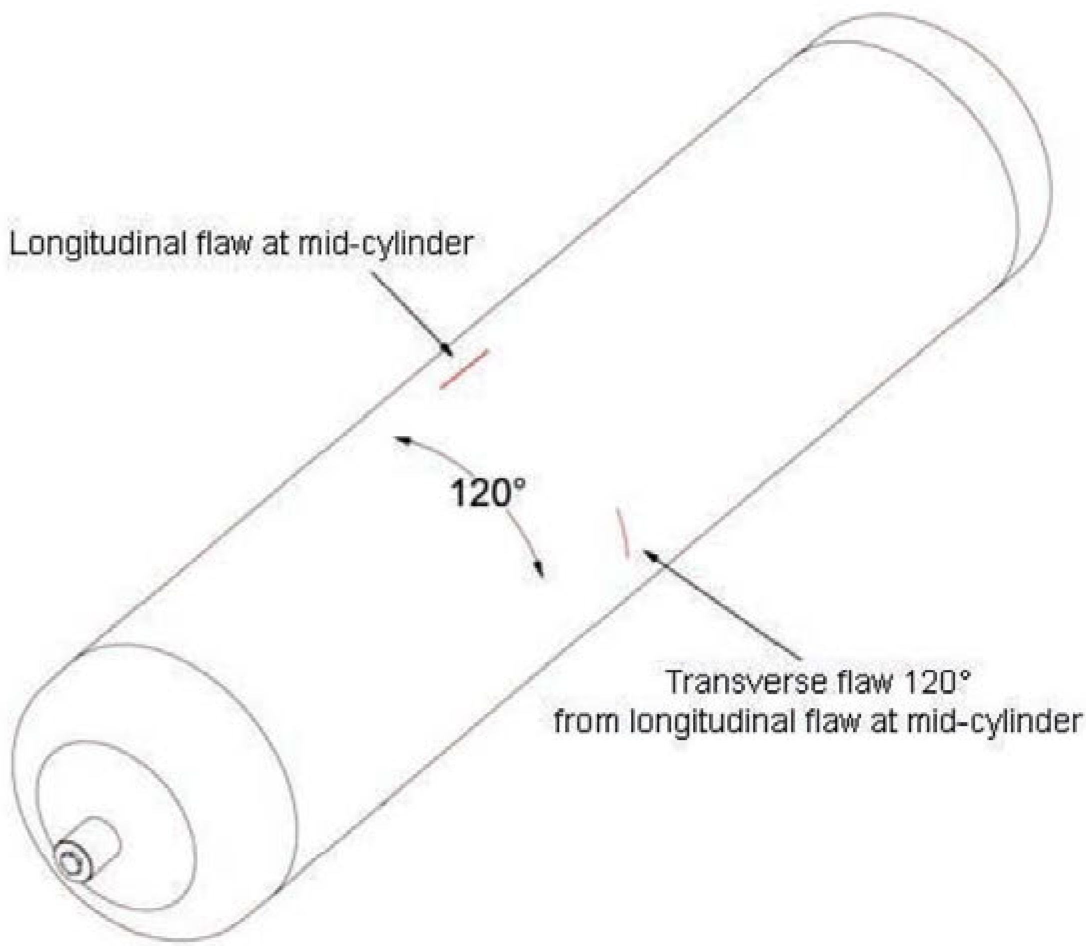

Figure 3 - Locations of Longitudinal and Transverse Flaws

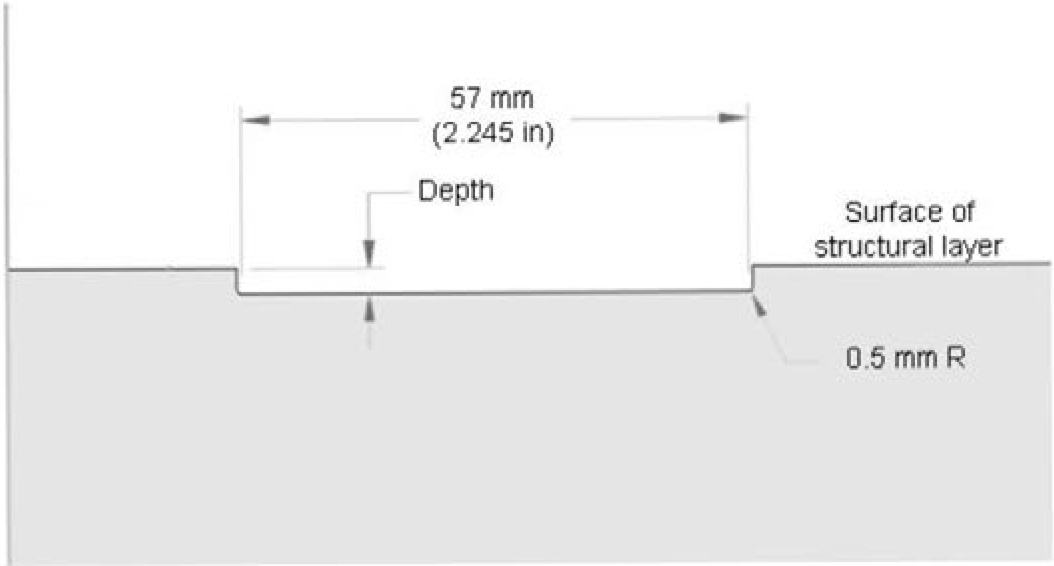

Figure 4 - Cross-Sectional View of Flaw

Table 2: Record of flaw dimensions ASME Flawed Cylinder Testing

Test Tank	SN [1]	Longitudinal Flaw Depth +/- 0.005 (inches)	Transverse Flaw Depth +/- 0.005 (inches)	Longitudinal glass overwrap removal Width	Longitudinal glass overwrap removal Length	Transverse glass overwrap removal Width	Transverse glass overwrap removal Length	Longitudinal Flaw Depth	Longitudinal Flaw Length	Transverse Flaw Depth	Transverse Flaw ~~width~~ length
1A	1007-002	0.090	0.090	.500	2.999	.500	2.990	.090	2.242	.092	2.242
1B	1007-003	0.090	0.090	.500	2.998	.510	2.995	.090	2.240	.089	2.243
1C	1007-001	0.090	0.090	.500	2.999	.500	3.000	.089	2.241	.089	2.245
2A	1007-009	0.135	0.135	.501	2.998	.500	2.490	.134	2.241	.136	2.241
2B	1007-004	0.135	0.135	.500	2.998	.500	2.997	.134	2.795	.135	2.240
2C	1007-015	0.135	0.135	.503	2.998	.500	2.991	.135	2.240	.135	2.241
3A	1007-011	0.180	0.180	.500	2.995	.500	2.998	.182	2.240	.181	2.243
3B	1007-012	0.180	0.180	.500	2.996	.500	2.997	.180	2.241	.181	2.240
3C	1007-013	0.180	0.180	.501	2.998	.500	2.998	.180	2.240	.181	2.241
4A	1007-005	0.050	0.050	.500	2.998	.500	2.997	.049	2.241	.050	2.245
4B	1007-006	0.050	0.050	.500	2.999	.500	3.000	.050	2.241	.051	2.245
4C	1007-010	0.050	0.050	.500	2.998	.500	3.000	.048	2.245	.051	2.241
5	1007-014	glass removal only	glass removal only	.500	2.998	.500	3.000	X	X	X	X

Figure 5 - Record of Flaw Depths, in Inches, after Machining

5 FATIGUE TEST

Eight of the thirteen tanks were cycled hydraulically to service pressure of 24.8 MPa (3600 psi) at room temperature to the number of cycles shown in Table 1. The maximum pressure was to be 24.8 +1.39/-0 MPa (3600 +200/-0 psi) and the minimum pressure was less than 2.48 MPa (360 psi). The test medium was water. Temperature of the composite laminate was measured and recorded at the mid-cylinder on each tank, and was nominally 41 °C (105 °F), with no tanks having exceeded 50 °C (122 °F) during cycling. The cycle frequency was recorded and was 3 to 4 pressure cycles per minute. No failures of the pressure vessels occurred during cycling. Results of the cycle testing are shown in Table 3. All of the flaws were visually inspected after cycling and no changes in the flaw were observed. An example of a flaw before and after 20,000 cycles is shown in Figure 6 and Figure 7.

Table 3 - Pressure Cycling Tests Results

Test Tank	SN [1]	Flaw Depth (% of structural thickness)	Cycles	Number of Successful cycles	Min pressure, MPa (psi) min recorded	Max pressure, MPa (psi) max recorded
5	1007-014	none	0	-	-	-
4A	1007-005	10%	0	-	-	-
1A	1007-002	20%	0	-	-	-
2A	1007-009	30%	0	-	-	-
3A	1007-011	40%	0	-	-	-
4C	1007-010	10%	10k	10,006	1.44 (209)	25.5 (3697)
1C	1007-001	20%	10k	10,006	1.44 (209)	25.5 (3697)
2C	1007-015	30%	10k	10,006	1.44 (209)	25.5 (3697)
3C	1007-013	40%	10k	10,000	1.94 (282)	25.2 (3660)
4B	1007-006	10%	20k	20,007	1.49 (216)	25.3 (3672)
1B	1007-003	20%	20k	20,007	1.49 (216)	25.3 (3672)
2B	1007-004	30%	20k	20,007	1.49 (216)	25.3 (3672)
3B	1007-012	40%	20k	20,006	1.68 (243)	25.2 (3658)

Note: Tanks 1C, 2C and 4C were cycled together and 1B, 2B and 4B were cycled together.

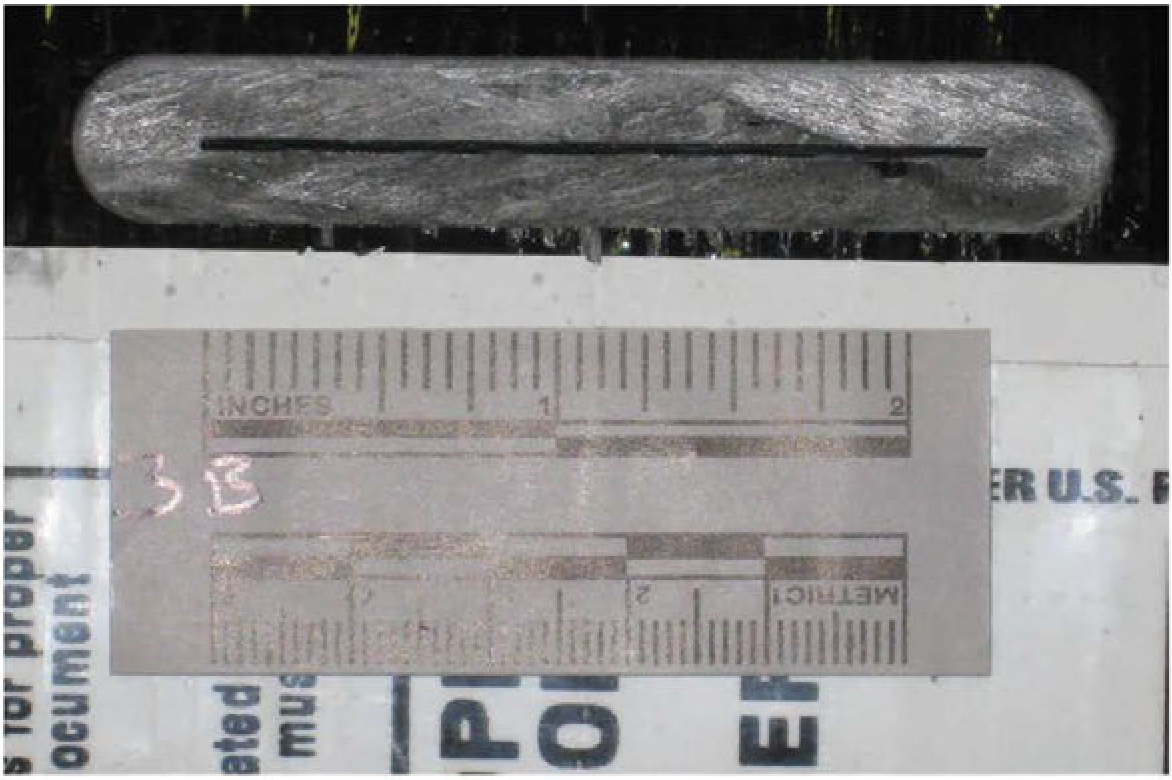

Figure 6 - Longitudinal Flaw in Tank 3B Before Cycling

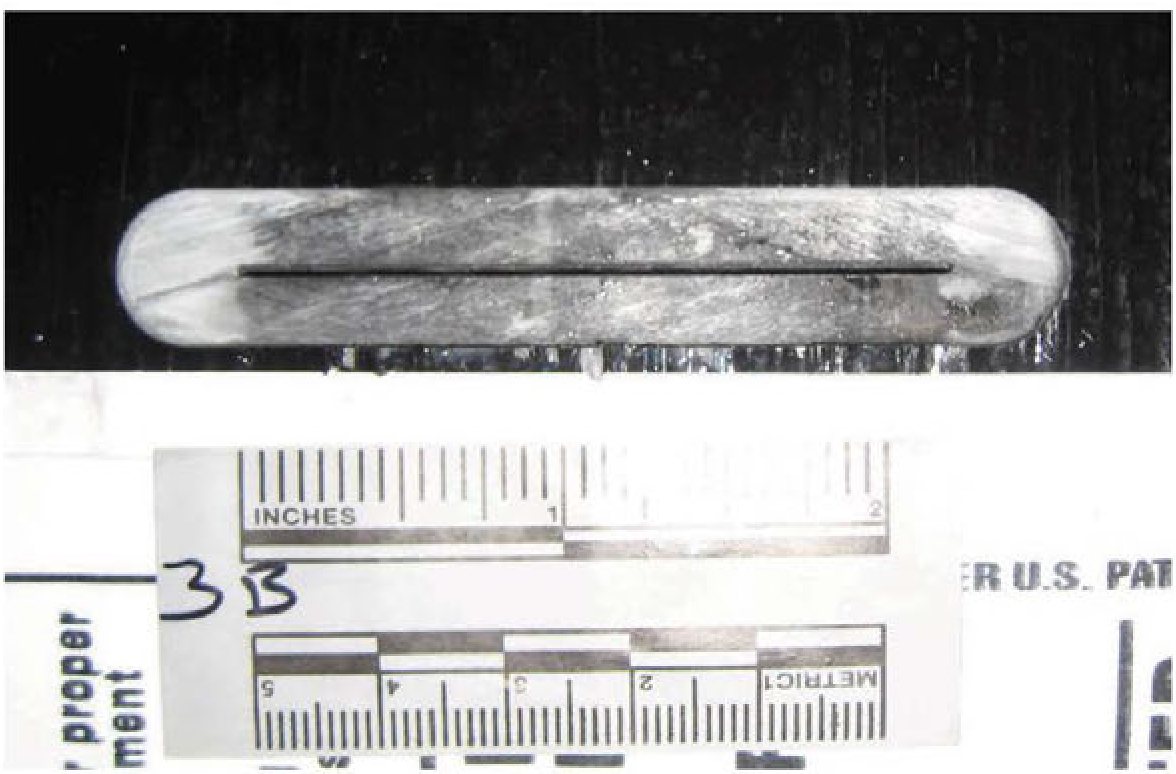

Figure 7 - Longitudinal Flaw in Tank 3B after 20,000 Cycles

6 BURST TESTING

Each cylinder was tested hydraulically with water to rupture at ambient conditions. The pressurization rate was less than 0.48 MPa/second (70 psi/second). The maximum pressure obtained and the burst initiation location were recorded and are shown in Table 4. The pressure versus time was recorded and is shown in Appendix B. Photographs of each cylinder after burst are shown in Appendix C. There are four photographs of each burst. The first two are overall views of the carcass and the last two are closer views of the flaw locations.

Table 4 - Summary of Burst Data

Order	Test Tank	SN [1]	Flaw Depth	Cycles	Burst, MPa (psi)	Location
1	5	1007-014	none	0	74.30 (10,776)	mid-cyl
2	4A	1007-005	10%	0	76.12 (11,041)	mid-cyl
3	1A	1007-002	20%	0	69.63 (10,099)	mid-cyl
4	2A	1007-009	30%	0	59.27 (8,597)	mid-cyl
5	3A	1007-011	40%	0	52.98 (7,685)	mid-cyl
6	4C	1007-010	10%	10k	71.46 (10,364)	mid-cyl
7	1C	1007-001	20%	10k	65.57 (9,510)	mid-cyl
8	2C	1007-015	30%	10k	63.54 (9,216)	mid-cyl
9	3C	1007-013	40%	10k	53.59 (7,773)	mid-cyl
10	4B	1007-006	10%	20k	65.37 (9,481)	mid-cyl
11	1B	1007-003	20%	20k	67.80 (9,834)	mid-cyl
12	2B	1007-004	30%	20k	60.29 (8,745)	mid-cyl
13	3B	1007-012	40%	20k	56.23 (8,156)	mid-cyl

[1] Chosen at random

7 RESULTS AND DISCUSSION

Burst data are listed in Table 5 and these pressures are graphed in Figure 8 and Figure 9. All bursts originated at the longitudinal flaw location mid-cylinder. This was expected since this flaw cut the hoop direction fibers preferentially, which resulted in a larger decrease in the burst performance than the transverse (circumferential) flaws.

Burst-to-operating pressure ratio was calculated as the ratio of the burst pressure to that of the service pressure, which in this case was 24.8 MPa (3600 psi).

$$burst - to - operating\ pressure\ ratio = \frac{Bust\ Pressure\ (MPa)}{24.8}$$

To compare the effect of flaw size and cycling with the burst pressures, the ratio between the burst pressure and the burst pressure of the tank without flaws and cycles was used.

$$Burst\ Retention = \frac{Burst\ Pressure\ (MPa)}{Burst\ Pressure\ of\ Tank\ 5\ (no\ flaws)}\ x\ 100\%$$

To compare the effect of cycling only, the ratio between the burst pressure and the burst pressure with the same flaw size but no cycles was used.

$$Cycle\ Retention = \frac{Burst\ Pressure\ (MPa)}{Burst\ Pressure\ of\ Tank\ with\ same\ flaw\ but\ no\ cycles}\ x\ 100\%$$

The burst history on this configuration was reviewed. The average of five bursts was 77.2 MPa (11,200 psi) and ranged from 71.7 MPa (10,400 psi) to 81.4 MPa (11,800 psi).

Tank 5 (no flaws or cycles baseline) burst at 74.3 MPa (10,776 psi) which is a burst-to-operating pressure ratio of 2.99. This burst was lower than the historical average but it was within the range of burst pressures, and even though there was no machined flaw in the structural layer, the glass overwrap had been removed in the location of the flaws. Tank 4A, which had flaws cut 10% through the structure, actually burst slightly higher at 76.1 MPa (11,041 psi). This higher burst pressure can be explained due to normal tank-to-tank variation in the manufacturing process and it should not be interpreted to mean that adding a small flaw increases burst performance. Other than this slight increase, generally a deeper flaw resulted in a lower burst pressure, which was expected. In addition, this trend of decreasing burst pressure with increasing flaw depth is observed when tanks that have been cycled 10,000 and 20,000 times are compared. This trend is clearly seen in the Burst Loss column of Table 5 and also in Figure 9. An exception to this was observed with a 2.23 MPa (324 psi) increase in burst pressure at 20,000 cycles for the 20% flaw over the 10% flaw.

The effect of cycling on a given flaw depth is shown in Figure 8. For a flaw 10% through the structural layer, the burst pressure decreases with increasing cycles. This indicates that, for a small flaw, cyclic fatigue loading does have an effect. However, the burst-to-operating pressure ratio was still 2.63 after 20,000 cycles. The indicated effect of cyclic loading on the deeper flaws was different. For the 40% flaw, cyclic fatigue loading actually increased the burst pressure when compared to the zero cycle tank with the same flaws. This trend was also observed with the 30% flaw and somewhat with the 20% flaw.

The explanation for this behavior with cycling is as follows. Flaws machined into the laminate with the 1 mm diameter carbide ball tool, even though there was a radius, resulted in a geometric stress riser. Upon loading, the stress at this point was concentrated until sudden fracture occurred which nucleated the burst of the vessel. For the two tanks that were cycled with the 40% flaws, a re-distribution of the stress concentration may have taken place. First, it is possible that the severity of the stress riser was mitigated by fatigue cracks originating at the locations of highest stresses. Secondly, these cracks formed by the cyclic loading may reduce the tendency of a sudden, intense fracture at the flaw that would nucleate the burst. In essence, it has been shown here that with severe flaws, cyclic loading to service pressure increases the pressure at burst. However, the differences in burst pressures between cyclic fatigue levels are small enough that some differences may be explained by scatter. It should be noted that continued cycling would eventually have a detrimental effect on the burst performance of the vessel.

Table 5 - Comparison of Burst Data

Test Tank	SN (1)	Flaw	Cycles	Burst, MPa (psi)	Location	BR (2)	Burst Retention(3)	Cycle Retention (4)
5	1007-014	none	0	74.30 (10,776)	mid-cyl	2.99	-	-
4A	1007-005	10%	0	76.12 (11,041)	mid-cyl	3.07	102.5%	-
1A	1007-002	20%	0	69.63 (10,099)	mid-cyl	2.81	93.7%	-
2A	1007-009	30%	0	59.27 (8,597)	mid-cyl	2.39	79.8%	-
3A	1007-011	40%	0	52.98 (7,685)	mid-cyl	2.13	71.3%	-
4C	1007-010	10%	10k	71.46 (10,364)	mid-cyl	2.88	96.2%	93.9%
1C	1007-001	20%	10k	65.57 (9,510)	mid-cyl	2.64	88.3%	94.2%
2C	1007-015	30%	10k	63.54 (9,216)	mid-cyl	2.56	85.5%	107.2%
3C	1007-013	40%	10k	53.59 (7,773)	mid-cyl	2.16	72.1%	101.1%
4B	1007-006	10%	20k	65.37 (9,481)	mid-cyl	2.63	88.0%	88.0%
1B	1007-003	20%	20k	67.80 (9,834)	mid-cyl	2.73	91.3%	97.4%
2B	1007-004	30%	20k	60.29 (8,745)	mid-cyl	2.43	81.2%	101.7%
3B	1007-012	40%	20k	56.23 (8,156)	mid-cyl	2.27	75.7%	106.1%

(1) Chosen at random

(2) Burst-to-operating pressure ratio (BR): Burst pressure / 24.8 MPa

(3) Burst Retention: Burst / 74.3 MPa (no-flaw burst tank)

(4) Cycle Retention: Burst / Burst of tank with same flaw but no cycles

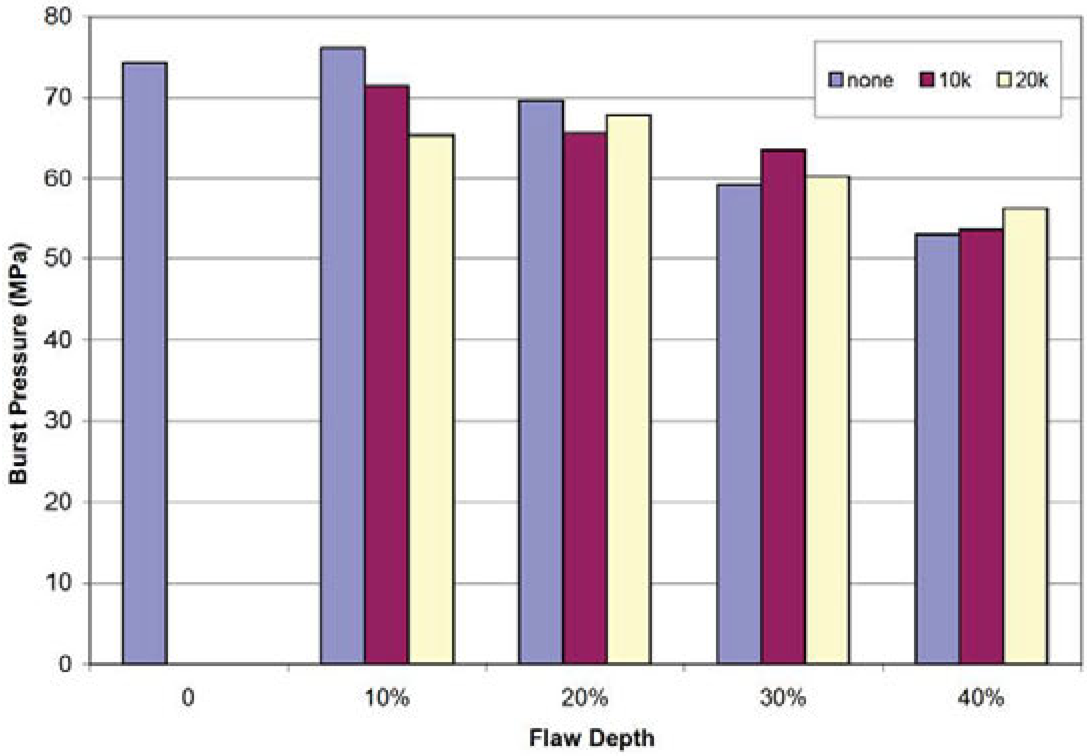

Figure 8 - Burst Pressure Versus Depth of Flaw and Cycling

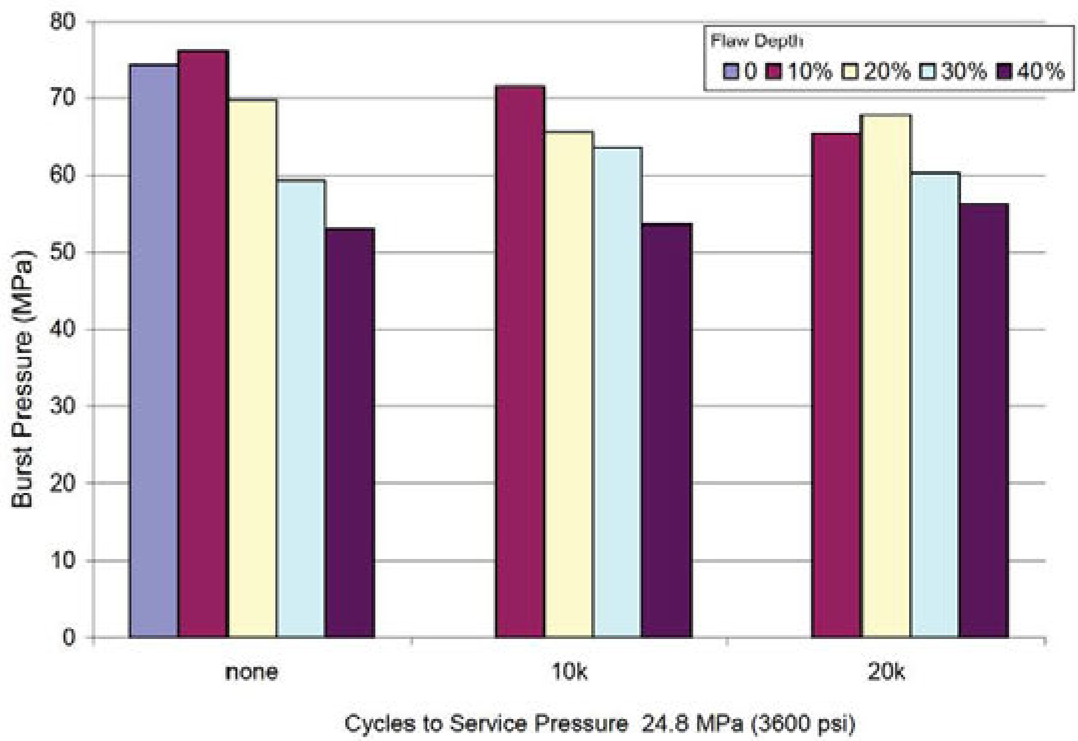

Figure 9 - Burst Pressure Versus Cycling and Depth of Flaw

8 SUMMARY AND CONCLUSIONS

The flawed cylinder test program has been completed as planned. None of the cylinders leaked or ruptured during the cycle testing. The burst results are reasonably consistent with expectations.

The lowest burst-to-operating pressure ratio was 2.13, which occurred with the 40% flaw with no cycles. The highest burst-to-operating pressure ratio was 3.07, which occurred with the 10% flaw with no cycles. The higher burst pressure of the 10% flaw tank over the tank without a flaw can be explained by normal manufacturing variation between tanks.

Burst pressure decreased as flaw depth increased. There is some indication that burst pressure will vary depending on the number of cycles and depth of cut, but the change in burst pressure over 20,000 cycles was insignificant compared with the initial loss in strength due to the flaw.

Even with deepest flaw, which is significantly deeper than flaws typically found in service, the resulting burst margin would still allow safe operation of the pressure vessel over a period of time.

The lack of significant additional strength loss with cycling gives a degree of confidence that even if flaws are not found immediately, the risk of a failure due to the flaw is low.

APPENDIX A

Flaws machined into the structure before testing

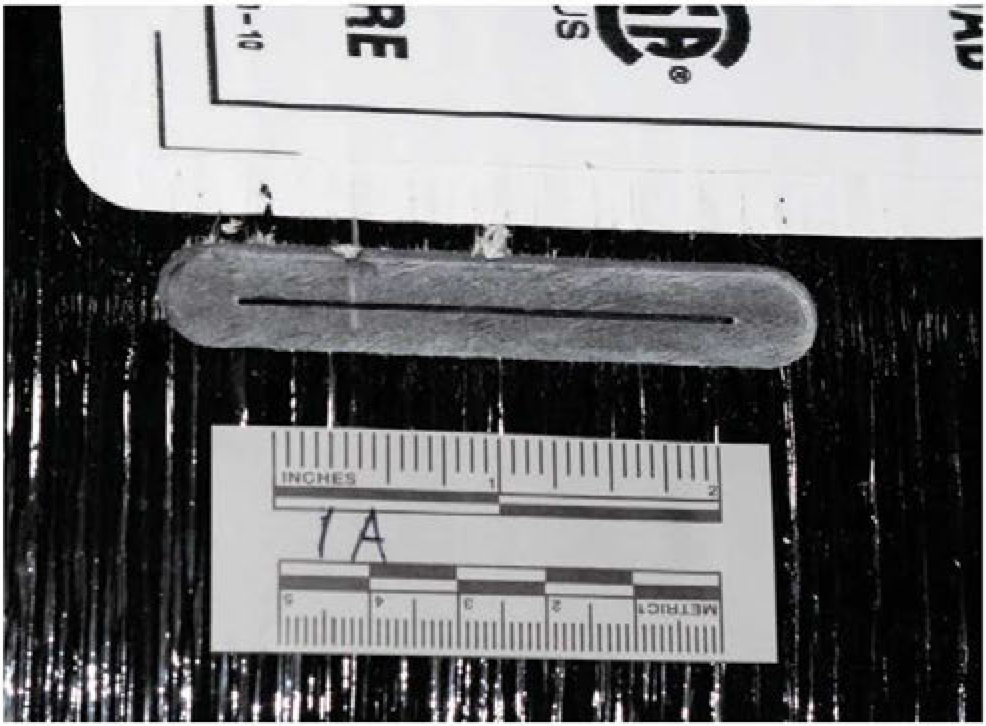

Figure A1: Tank 1A, Longitudinal Flaw Direction

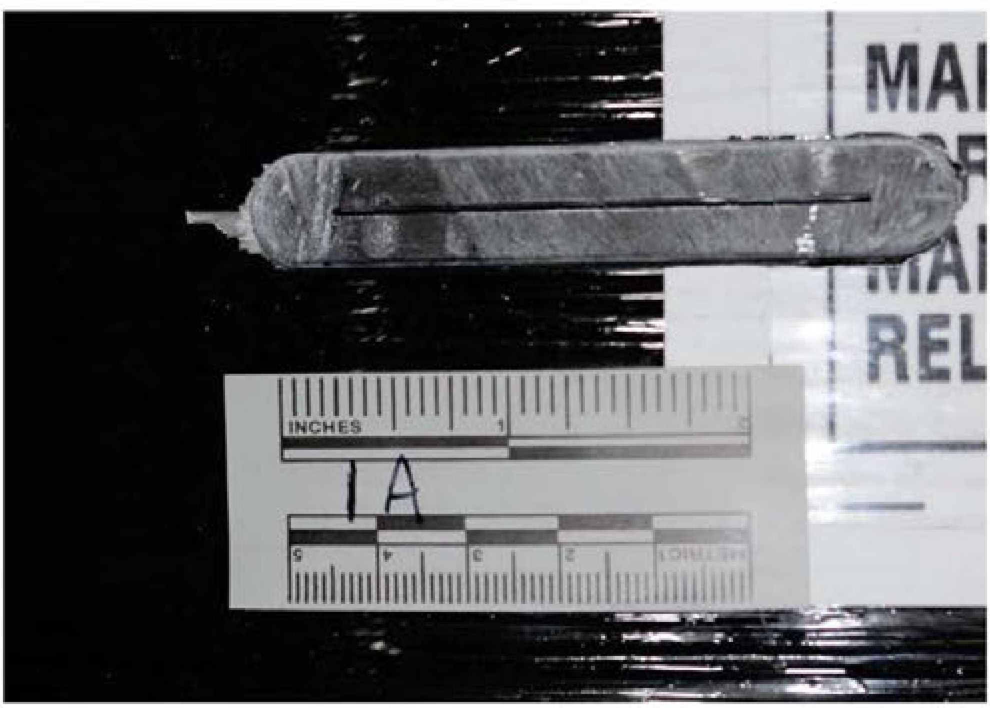

Figure A2: Tank 1A, Transverse Flaw Direction

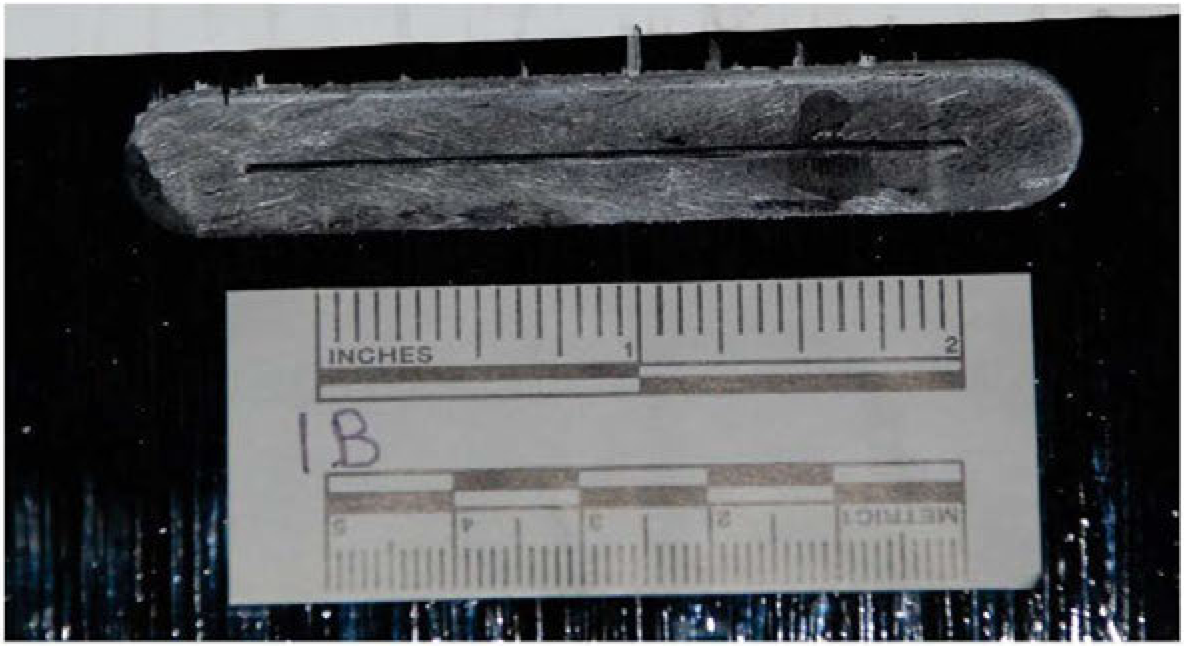

Figure A3: Tank 1B, Longitudinal Flaw Direction

Figure A4: Tank 1B, Transverse Flaw Direction

Figure A5: Tank 1C, Longitudinal Flaw Direction

Figure A6: Tank 1C, Transverse Flaw Direction

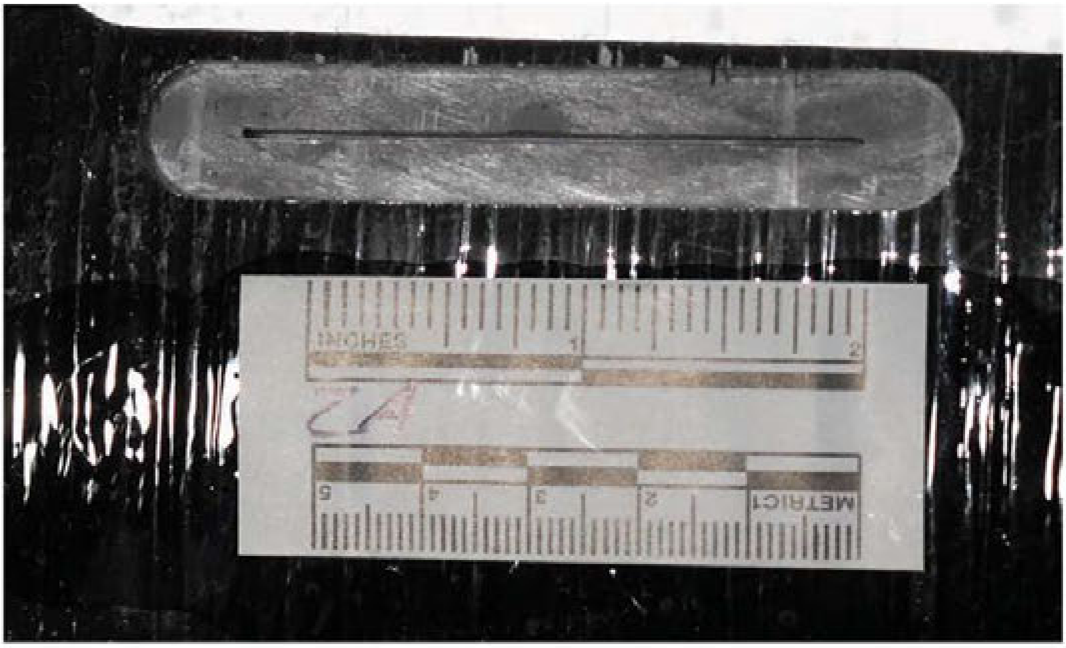

Figure A7: Tank 2A, Longitudinal Flaw Direction

Figure A8: Tank 2A, Transverse Flaw Direction

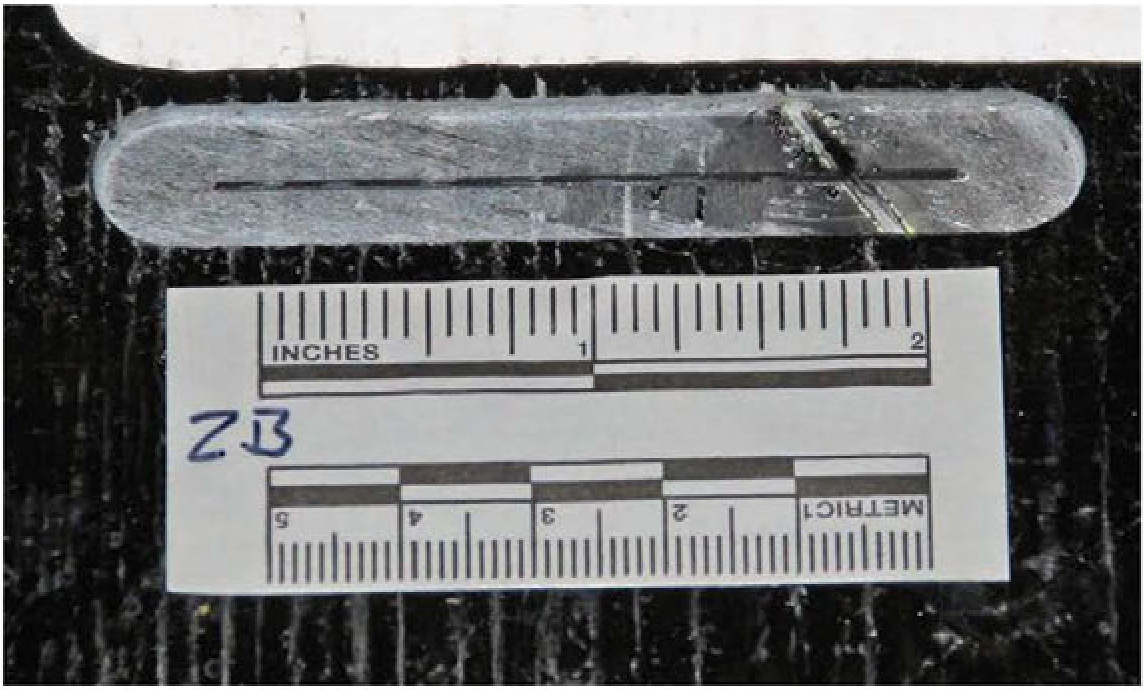

Figure A9: Tank 2B, Longitudinal Flaw Direction

Figure A10: Tank 2B, Transverse Flaw Direction

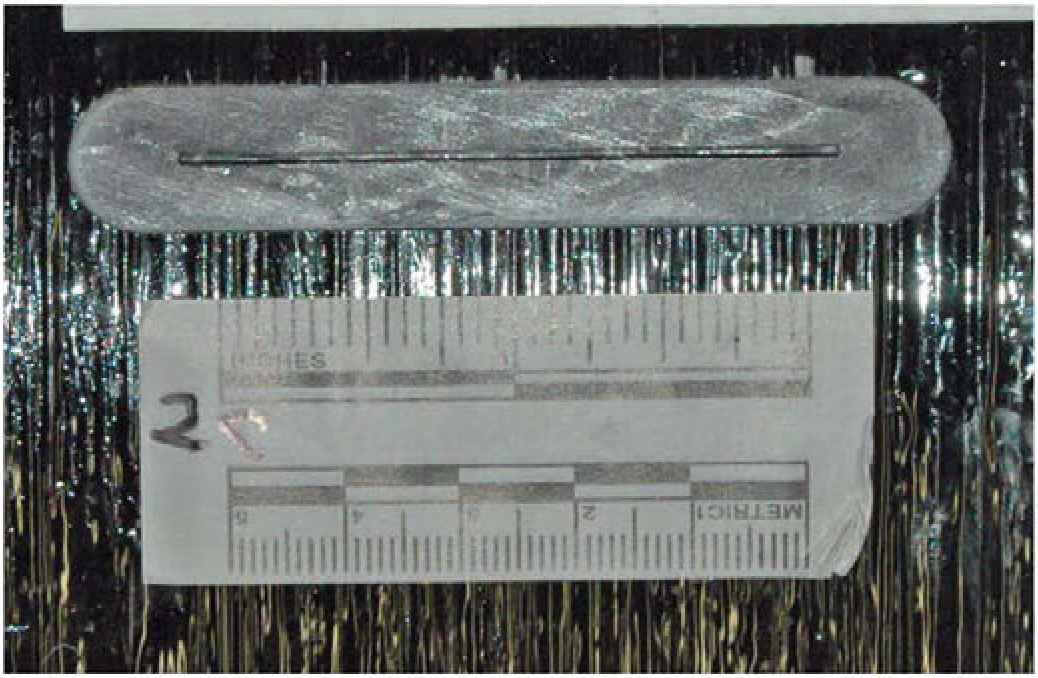

Figure A11: Tank 2C, Longitudinal Flaw Direction

Figure A12: Tank 2C, Transverse Flaw Direction

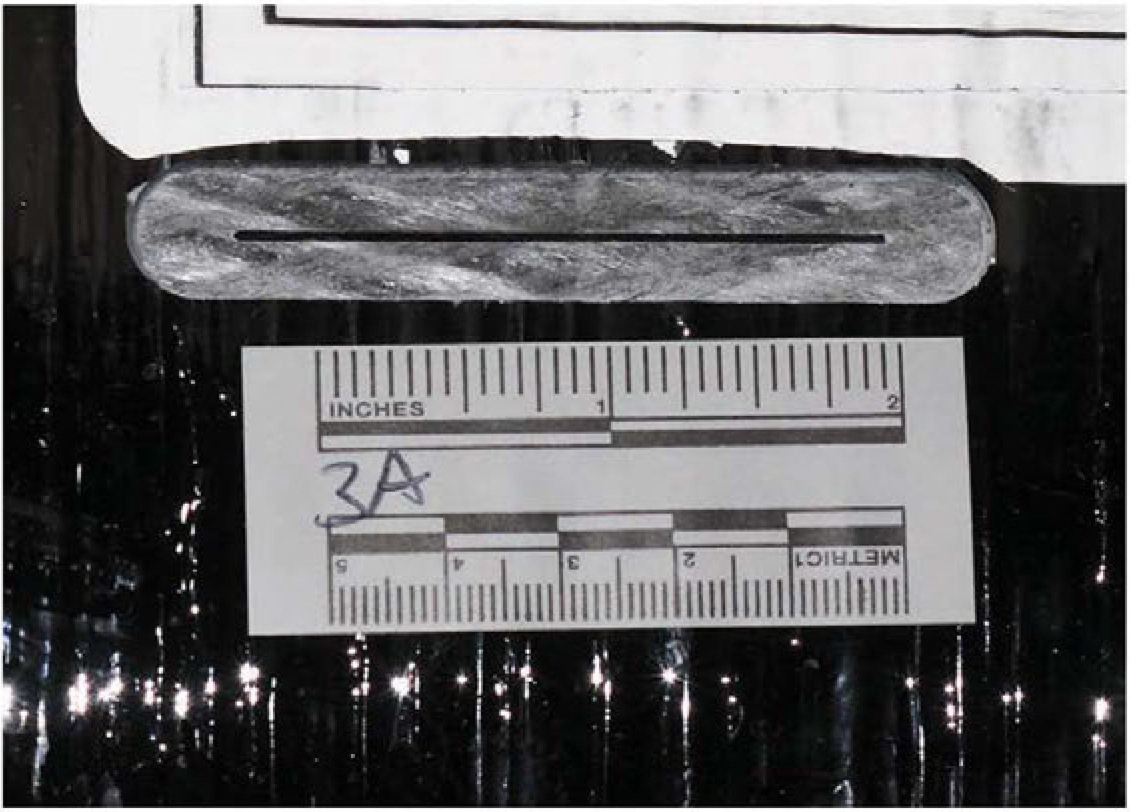

Figure A13: Tank 3A, Longitudinal Flaw Direction

Figure A14: Tank 3A, Transverse Flaw Direction

Figure A15: Tank 3B, Longitudinal Flaw Direction

Figure A16: Tank 3B, Transverse Flaw Direction

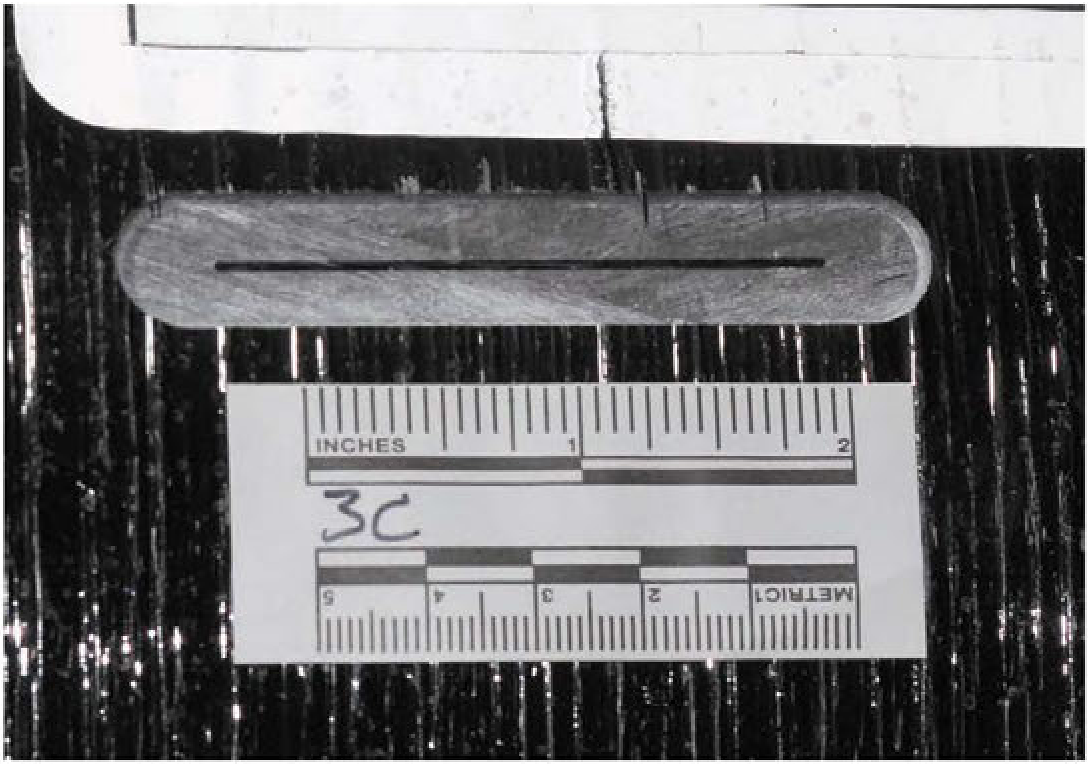

Figure A17: Tank 3C, Longitudinal Flaw Direction

Figure A18: Tank 3C, Transverse Flaw Direction

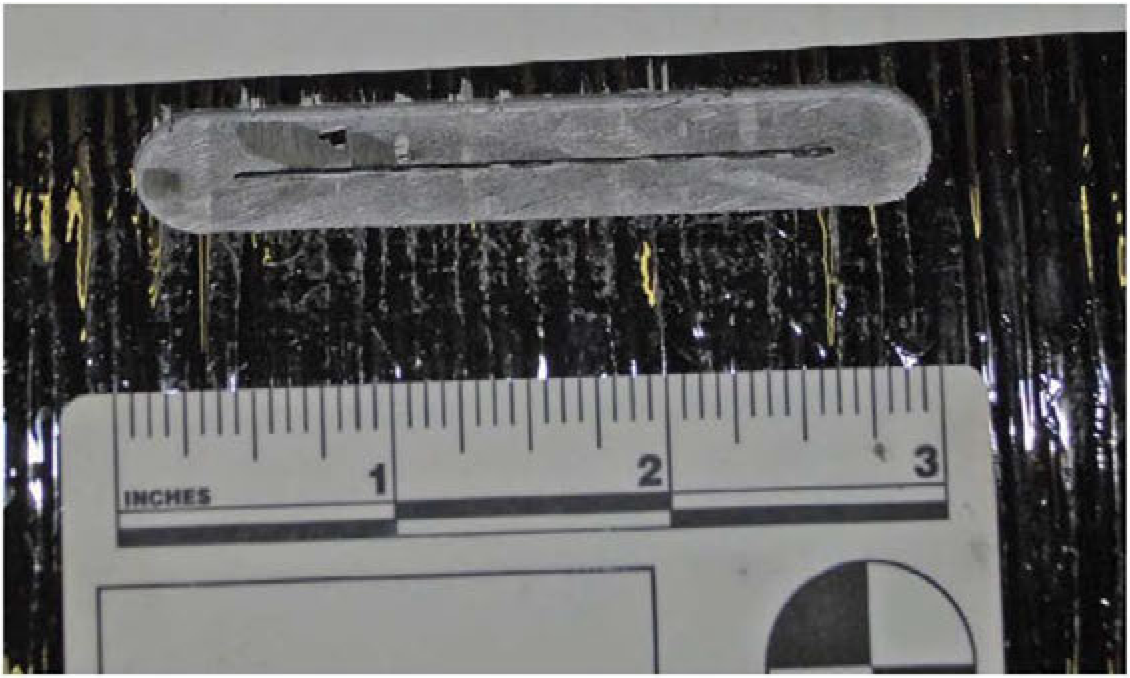

Figure A19: Tank 4A, Longitudinal Flaw Direction

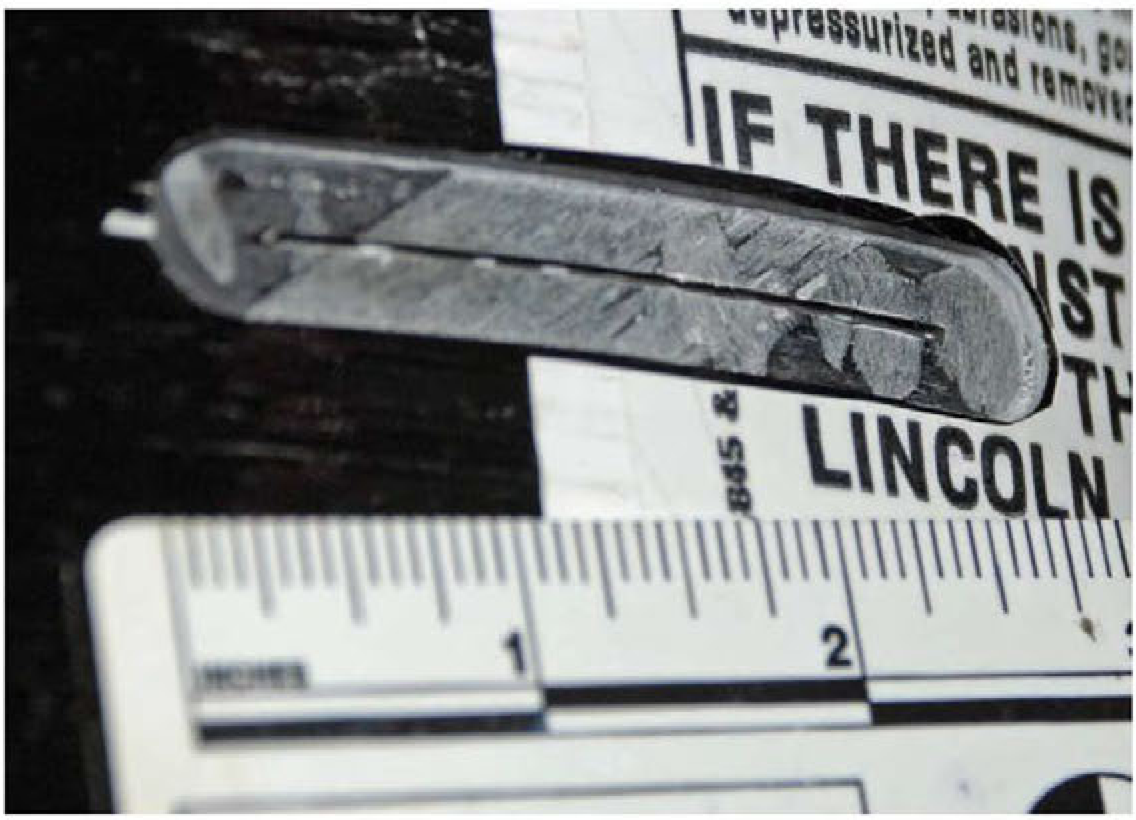

Figure A20: Tank 4A, Transverse Flaw Direction

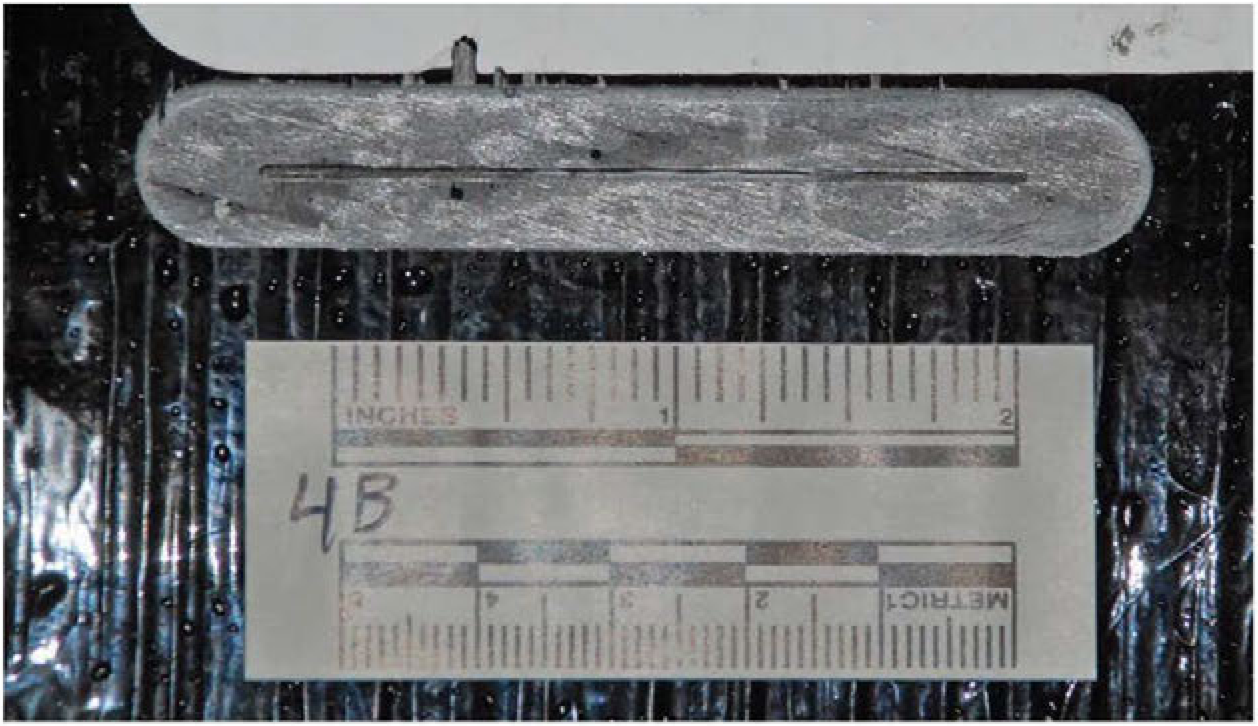

Figure A21: Tank 4B, Longitudinal Flaw Direction

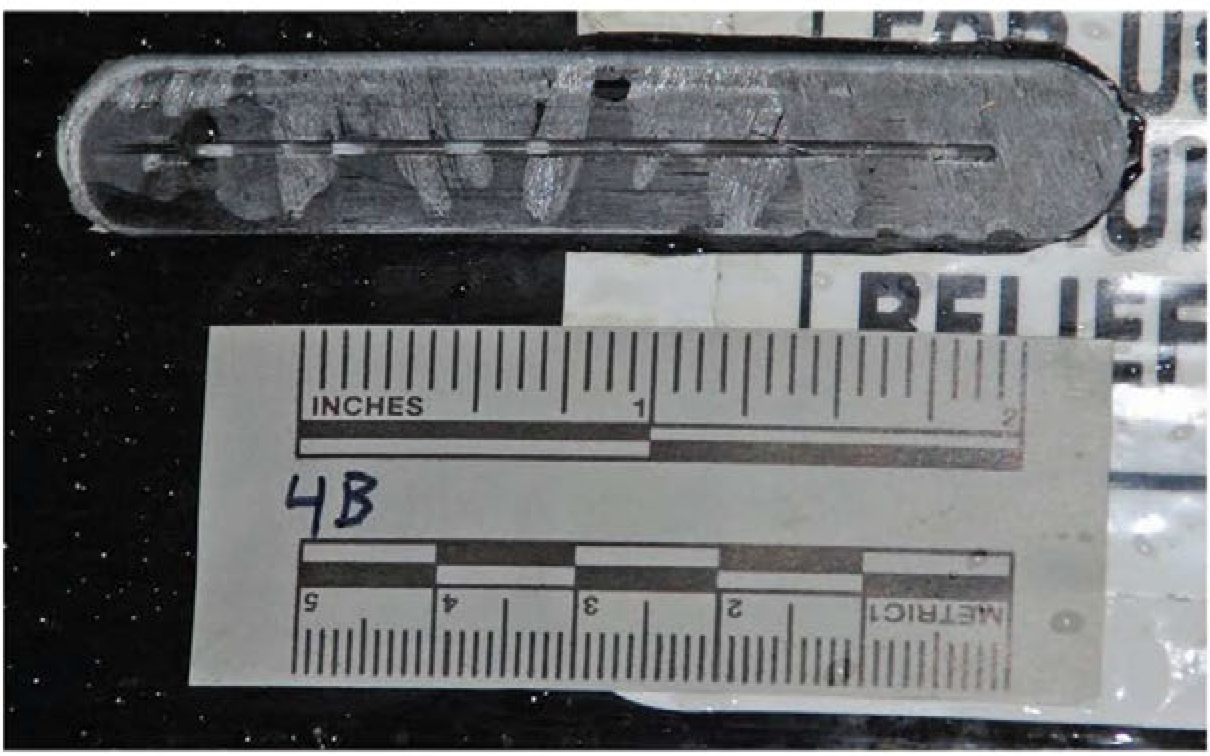

Figure A22: Tank 4B, Transverse Flaw Direction

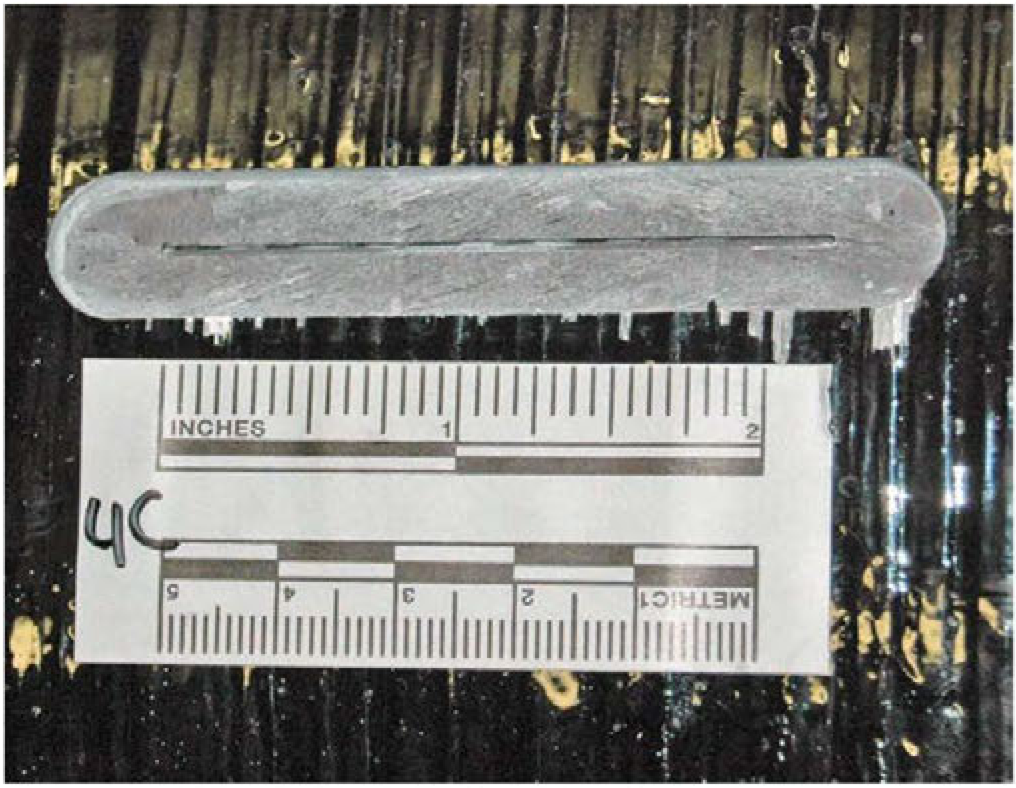

Figure A23: Tank 4C, Longitudinal Flaw Direction

Figure A24: Tank 4C, Transverse Flaw Direction

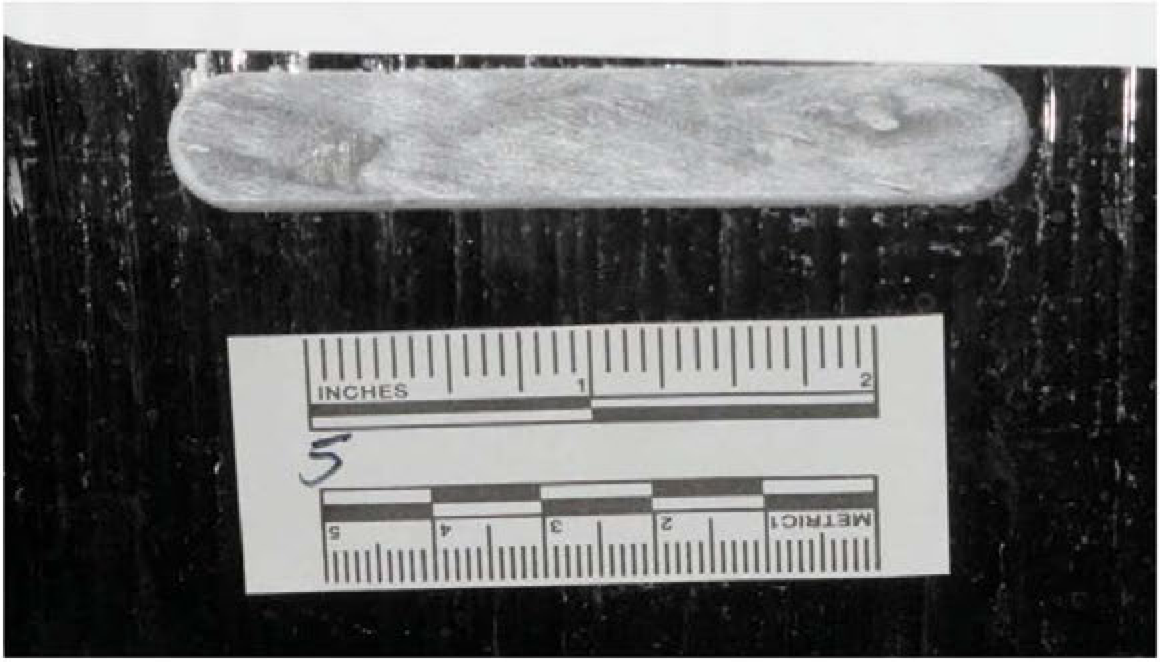

Figure A25: Tank 5, Longitudinal Glass Removal Only

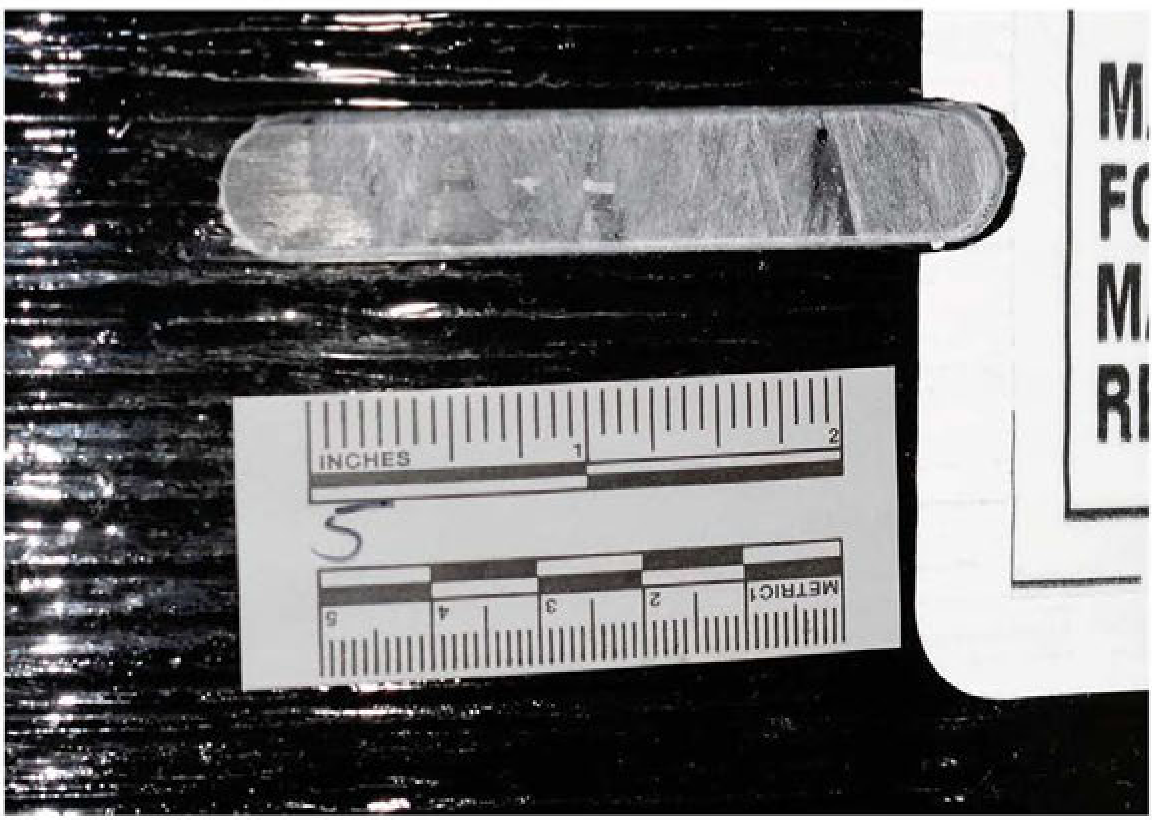

Figure A26: Tank 5, Transverse Glass Removal Only

APPENDIX B

Hydrostatic burst test reports

Hydrostatic Burst Test Report

LINCOLN COMPOSITES
A Member of Hexagon Composites Group

LPS: 98033 Rev.	AD	***TR#***	2130
Test Date:	Monday, June 22, 2009		
Test Time:	10:04 AM		
Part Number:	240075-023		
Serial Number:	1007-014		
Pressure Range (PSI):	3600		
Burst Pressure (PSI):	**10776**		
Minimum Burst (PSI):	0		
Operator:	Richards		
Witness:			
Burst Location:	Mid Cyl		

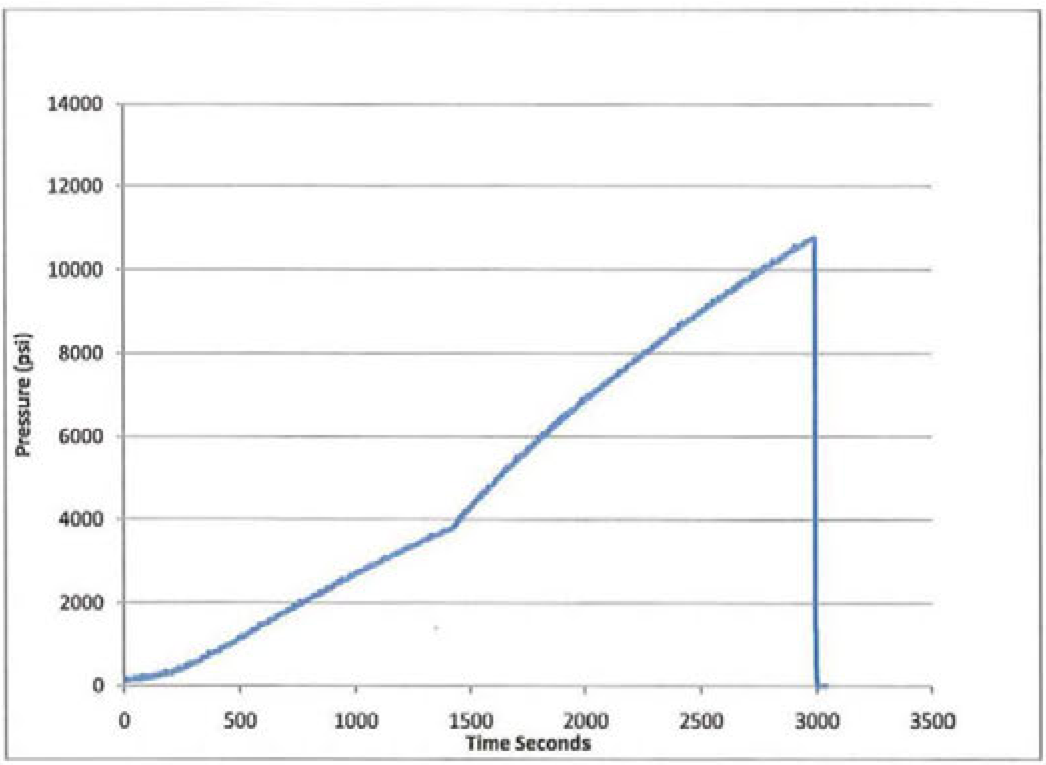

Figure B1: Pressure vs. Time -Tank 5, No Flaw, No Cycles

Hydrostatic Burst Test Report

LINCOLN COMPOSITES
A Member of Hexagon Composites Group

LPS: 98033 Rev.	AD	***TR#***	2130
Test Date:	Monday, June 22, 2009		
Test Time:	11:10 AM		
Part Number:	240075-023		
Serial Number:	1007-005		
Pressure Range (PSI):	3600		
Burst Pressure (PSI):	**11041**		
Minimum Burst (PSI):	0		
Operator:	Richards		
Witness:			
Burst Location:	Mid-cyl		

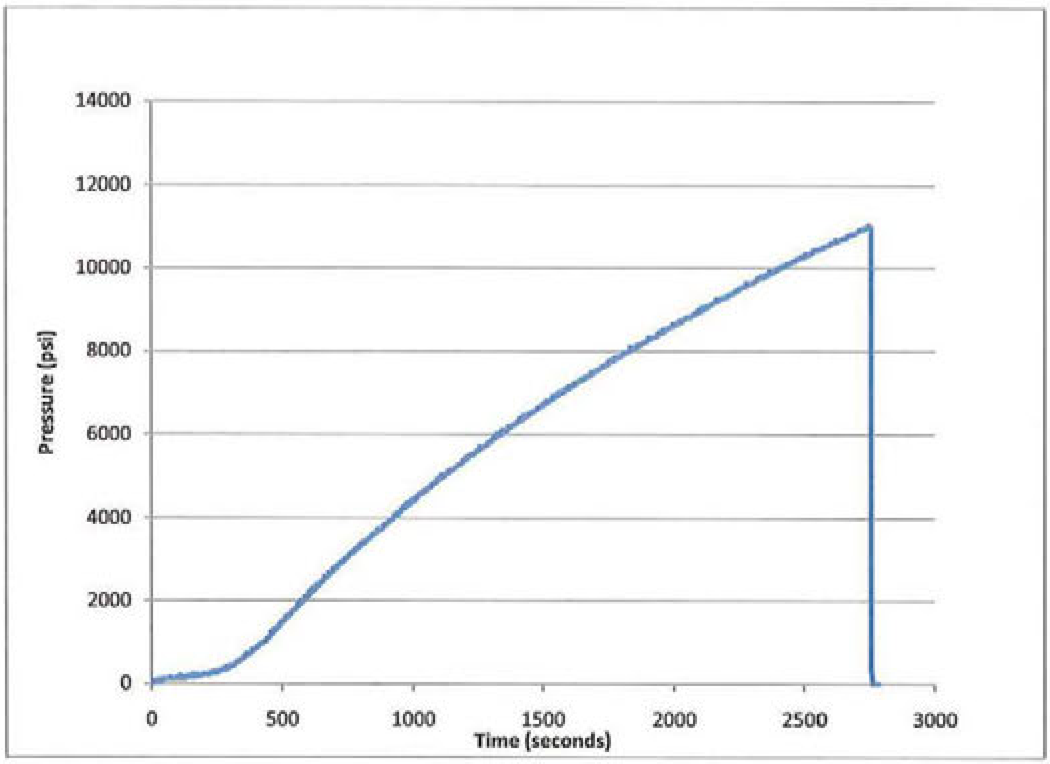

Figure B2: Pressure vs. Time - Tank 4A, 10% Flaw, No Cycles

Hydrostatic Burst Test Report

LINCOLN COMPOSITES
A Member of Hexagon Composites Group

LPS: 98033 Rev.	AD
Test Date:	Monday, June 22, 2009
Test Time:	10:35 AM
Part Number:	240075-023
Serial Number:	1007-002
Pressure Range (PSI):	3600
Burst Pressure (PSI):	**10099**
Minimum Burst (PSI):	0
Operator:	Richards

TR# 2130

Witness: ______________________

Burst Location: Md-cyl

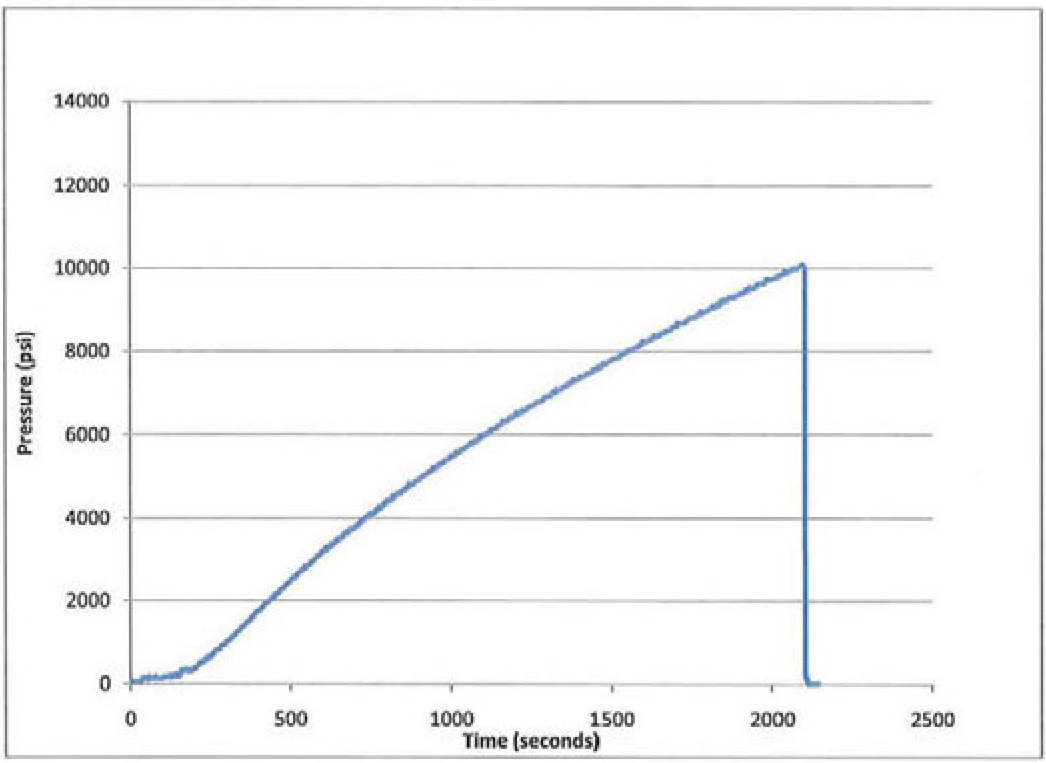

Figure B3: Pressure vs. Time - Tank 1A, 20% Flaw, No Cycles

Hydrostatic Burst Test Report

LINCOLN COMPOSITES
A Member of Hexagon Composites Group

LPS: 98033 Rev. AD
Test Date: Monday, June 22, 2009
Test Time: 11:00 AM
Part Number: 240075-023
Serial Number: 1007-009
Pressure Range (PSI): 3600
Burst Pressure (PSI): **8597**
Minimum Burst (PSI): 0
Operator: Richards

TR# 2130

Witness: ______________________

Burst Location: Mid-cyl

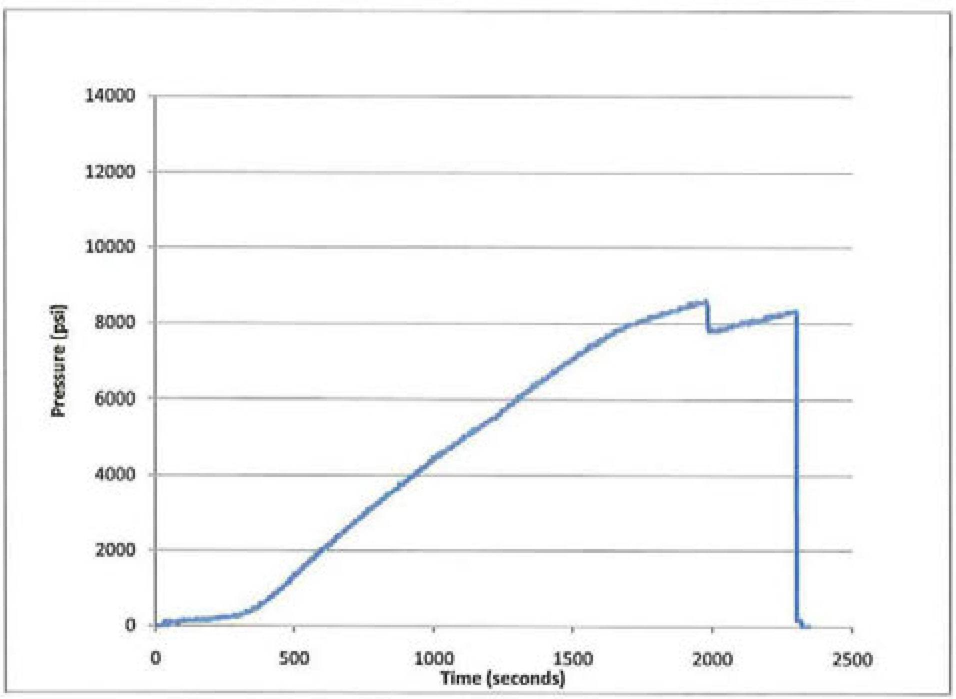

Figure B4: Pressure vs. Time - Tank 2A, 30% Flaw, No Cycles

Hydrostatic Burst Test Report

LINCOLN COMPOSITES
A Member of Hexagon Composites Group

LPS: 98033 Rev.	AD	***TR#***	2130
Test Date:	Monday, June 22, 2009		
Test Time:	9:15 AM		
Part Number:	240075-023		
Serial Number:	1007-011		
Pressure Range (PSI):	3600		
Burst Pressure (PSI):	**7685**		
Minimum Burst (PSI):	0		
Operator:	Richards		

Witness: ____________________

Burst Location: Mid-cyl

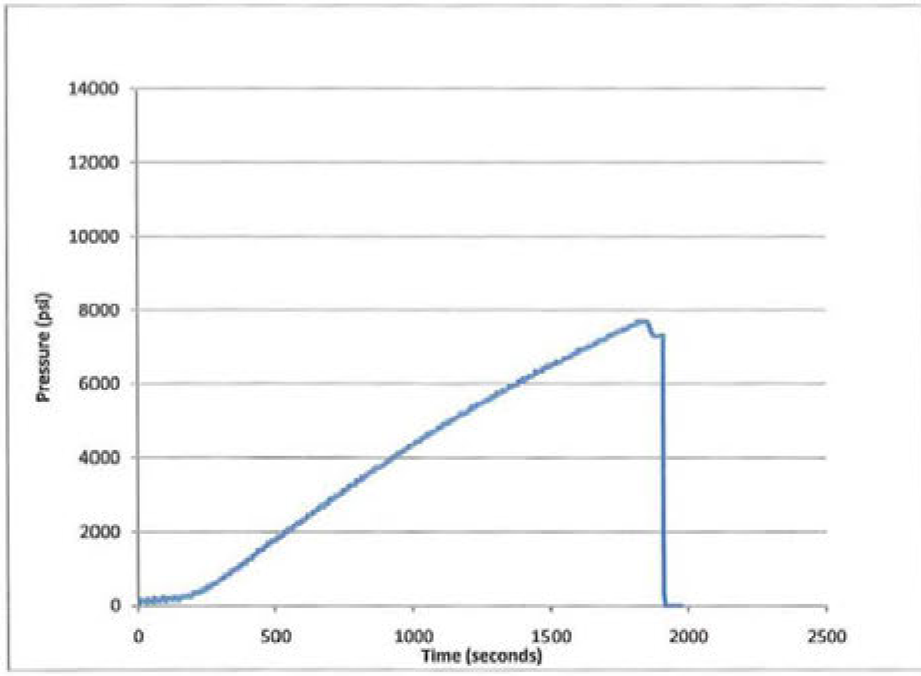

Figure B5: Pressure vs. Time - Tank 3A, 40% Flaw, No Cycles

Hydrostatic Burst Test Report

LINCOLN COMPOSITES
A Member of Hexagon Composites Group

LPS: 98033 Rev.	na	***TR#***	2130
Test Date:	Tuesday, July 14, 2009		
Test Time:	1:23 PM		
Part Number:	240075-023		
Serial Number:	1007-010		
Pressure Range (PSI):	3600		
Burst Pressure (PSI):	**10364**		
Minimum Burst (PSI):	0		
Operator:	573		

Witness: ______________________

Burst Location: Mid-cyl

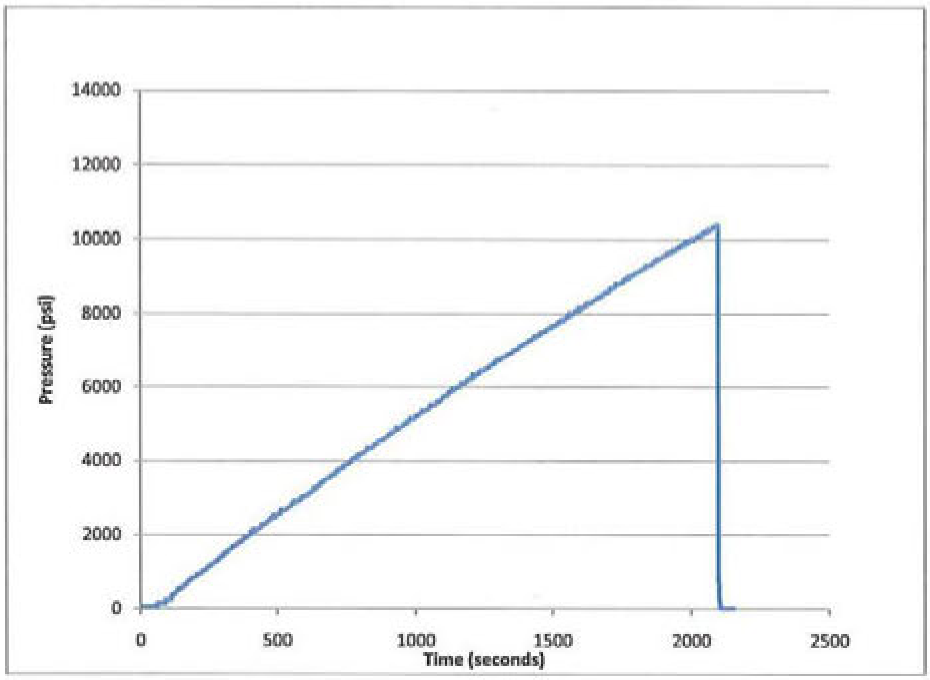

Figure B6: Pressure vs. Time - Tank 4C, 10% Flaw, No Cycles

Hydrostatic Burst Test Report

LINCOLN COMPOSITES
A Member of Hexagon Composites Group

LPS: 98033 Rev.	na	***TR#***	2130
Test Date:	Tuesday, July 14, 2009		
Test Time:	1:00 PM		
Part Number:	240075-023		
Serial Number:	1007-001		
Pressure Range (PSI):	3600		
Burst Pressure (PSI):	**9510**		
Minimum Burst (PSI):	0		
Operator:	573		

Witness: ____________________

Burst Location: Mid-cyl

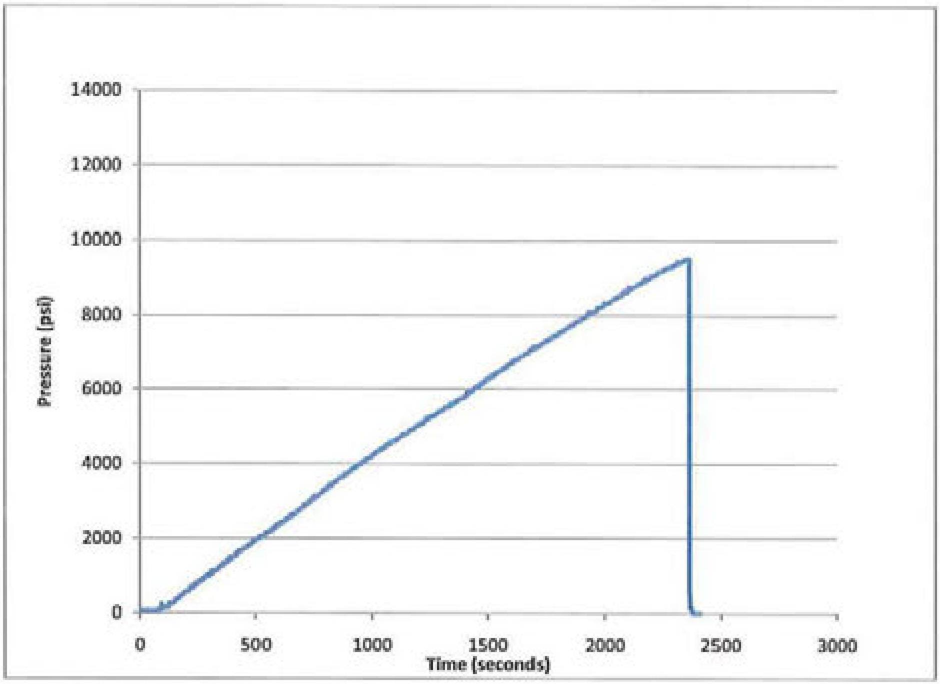

Figure B7: Pressure vs. Time - Tank 1C, 20% Flaw, No Cycles

Hydrostatic Burst Test Report

LINCOLN COMPOSITES
A Member of Hexagon Composites Group

LPS: 98033 Rev.	NA	***TR#***	2130
Test Date:	Tuesday, July 14, 2009		
Test Time:	12:37 PM		
Part Number:	240075-023		
Serial Number:	1007-015		
Pressure Range (PSI):	3600		
Burst Pressure (PSI):	**9216**		
Minimum Burst (PSI):	0		
Operator:	573		

Witness: ______________________

Burst Location: Mid-cyl

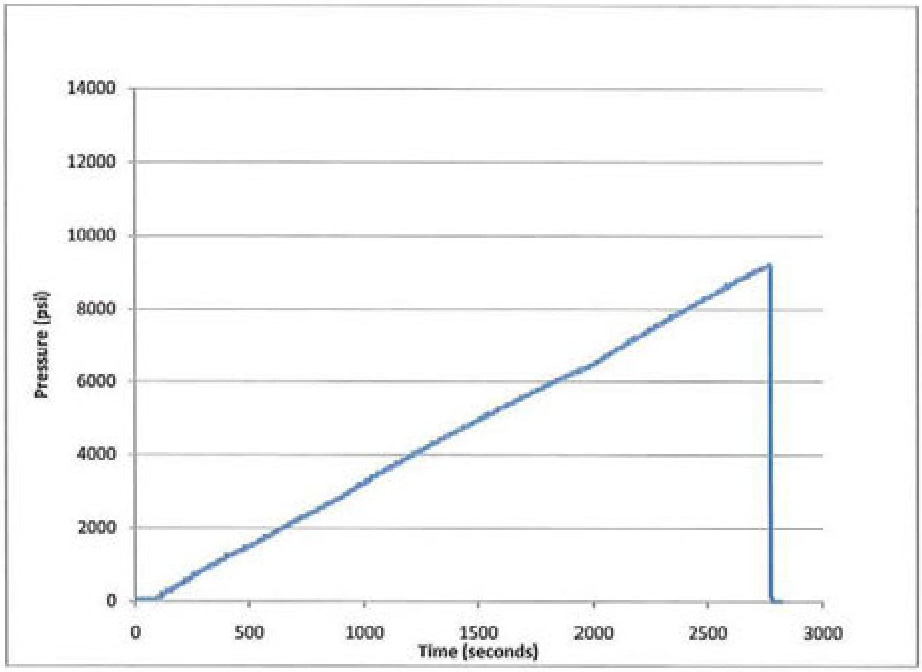

Figure B8: Pressure vs. Time - Tank 2C, 30% Flaw, No Cycles

Hydrostatic Burst Test Report

LINCOLN COMPOSITES
A Member of Hexagon Composites Group

LPS: 98033 Rev.		***TR#*** 2130
Test Date:	Thursday, July 09, 2009	
Test Time:	4:22 PM	
Part Number:	240075-23	
Serial Number:	1007-013	
Pressure Range (PSI):	3600	
Burst Pressure (PSI):	**7773**	
Minimum Burst (PSI):	0	
Operator:	513	

Witness: ______________________

Burst Location: Mid-Cyl

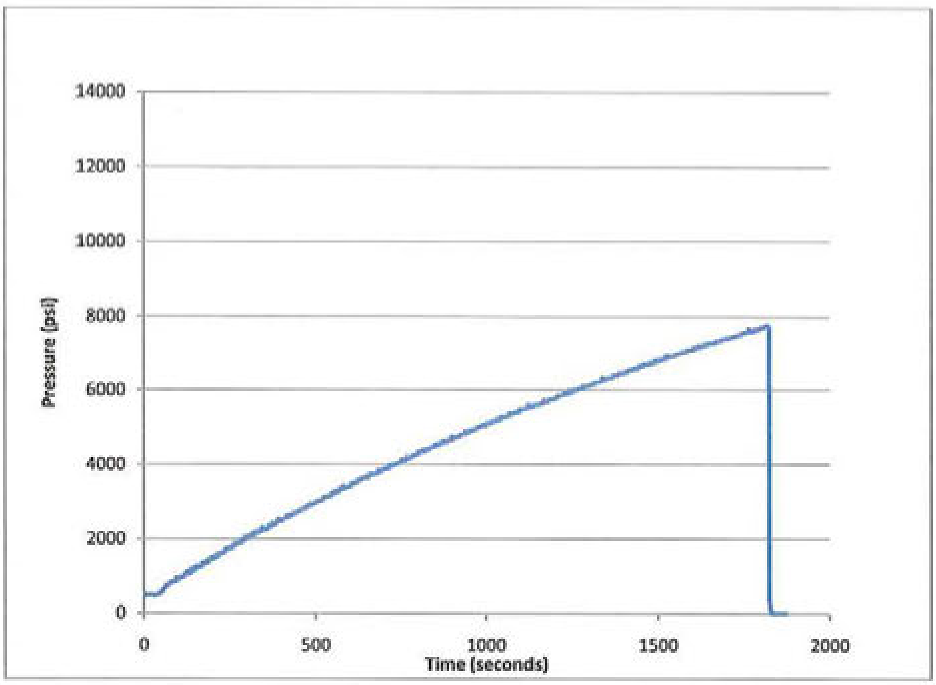

Figure B9: Pressure vs. Time - Tank 3C, 40% Flaw, No Cycles

Hydrostatic Burst Test Report

LINCOLN COMPOSITES
A Member of Hexagon Composites Group

LPS: 98033 Rev.	NA	*TR#*	2130
Test Date:	Tuesday, July 28, 2009		
Test Time:	7:56 AM		
Part Number:	240075-23		
Serial Number:	1007-006		
Pressure Range (PSI):	3600		
Burst Pressure (PSI):	**9481**		
Minimum Burst (PSI):	0		
Operator:	573		

Witness: ______________________

Burst Location: Mid-cyl

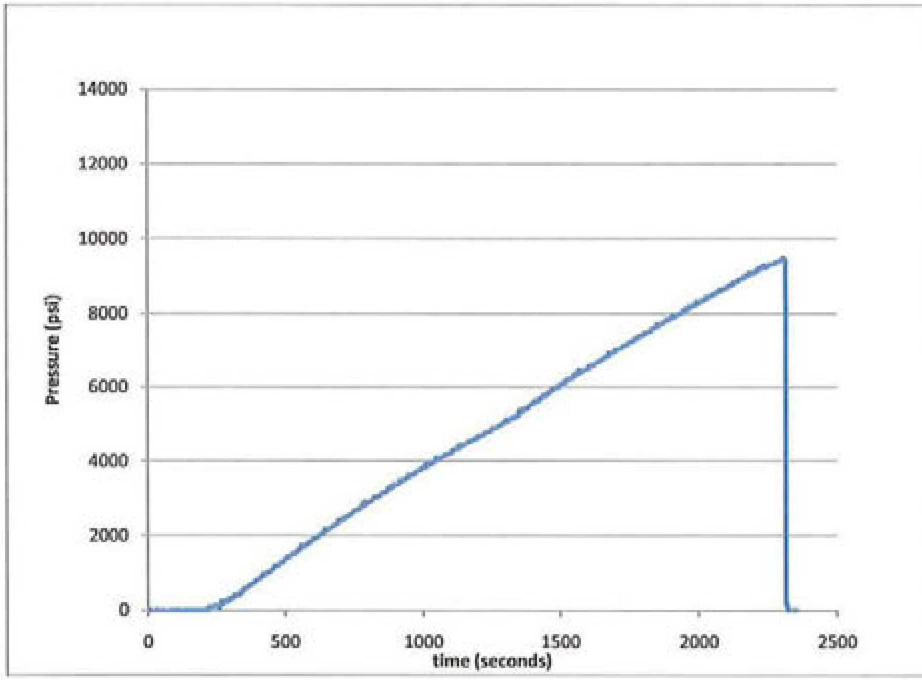

Figure B10: Pressure vs. Time - Tank 4B, 10% Flaw, No Cycles

Hydrostatic Burst Test Report

LINCOLN COMPOSITES
A Member of Hexagon Composites Group

LPS: 98033 Rev.	na	***TR#***	2130
Test Date:	Wednesday, July 29, 2009		
Test Time:	7:02 AM		
Part Number:	240075-023		
Serial Number:	1007-003		
Pressure Range (PSI):	3600		
Burst Pressure (PSI):	9834		
Minimum Burst (PSI):	0		
Operator:	573		

Witness: ____________________

Burst Location: Mid-cyl

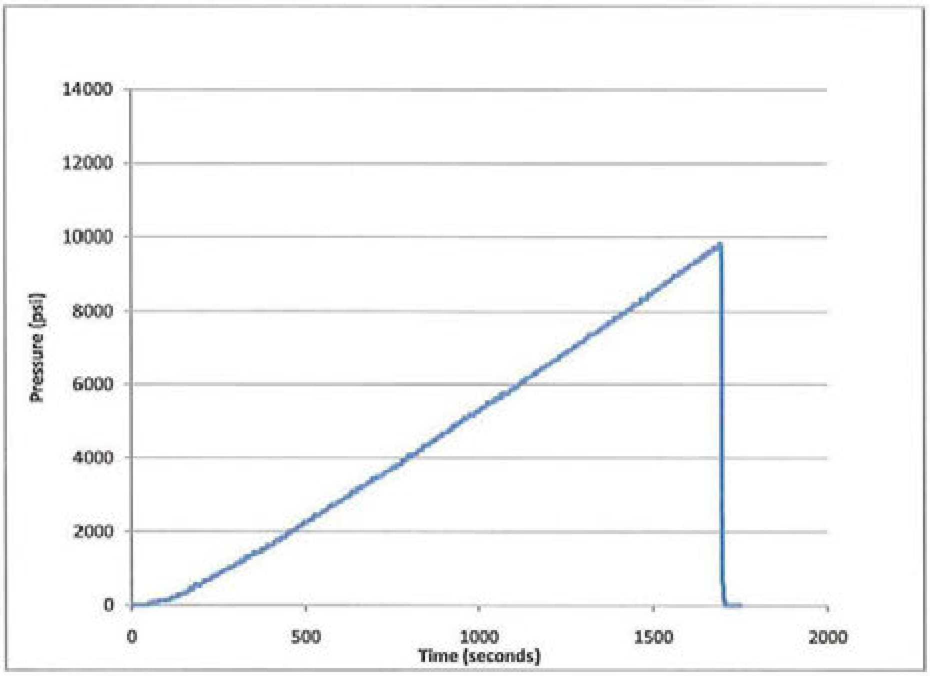

Figure B11: Pressure vs. Time - Tank 1B, 20% Flaw, No Cycles

Hydrostatic Burst Test Report

LINCOLN COMPOSITES
A Member of Hexagon Composites Group

LPS: 98033 Rev.	na	*TR#*	2130
Test Date:	Wednesday, July 29, 2009		
Test Time:	7:25 AM		
Part Number:	240075-023		
Serial Number:	1007-004		
Pressure Range (PSI):	3600		
Burst Pressure (PSI):	**8745**		
Minimum Burst (PSI):	0		
Operator:	573		

Witness: ______________________

Burst Location: mid-cyl

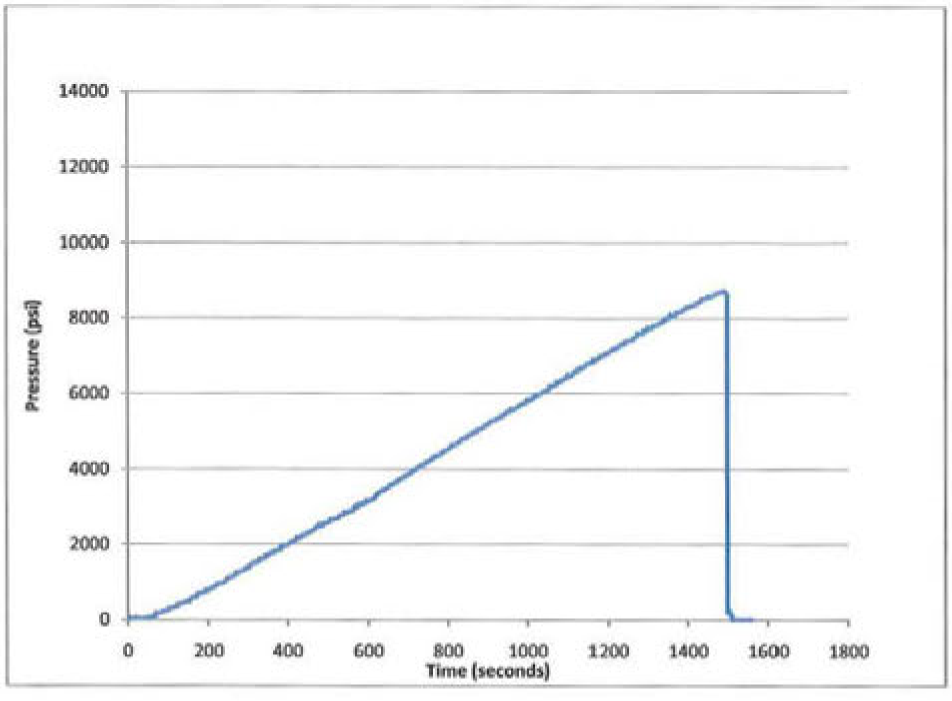

Figure B12: Pressure vs. Time - Tank 2B, 30% Flaw, No Cycles

Hydrostatic Burst Test Report

LINCOLN COMPOSITES
A Member of Hexagon Composites Group

LPS: 98033 Rev.	na	***TR#***	2130
Test Date:	Monday, July 20, 2009		
Test Time:	7:43 AM		
Part Number:	240075-023		
Serial Number:	1007-012		
Pressure Range (PSI):	3600		
Burst Pressure (PSI):	**8156**		
Minimum Burst (PSI):	0		
Operator:	573		
Witness:			
Burst Location:	Mid-cyl		

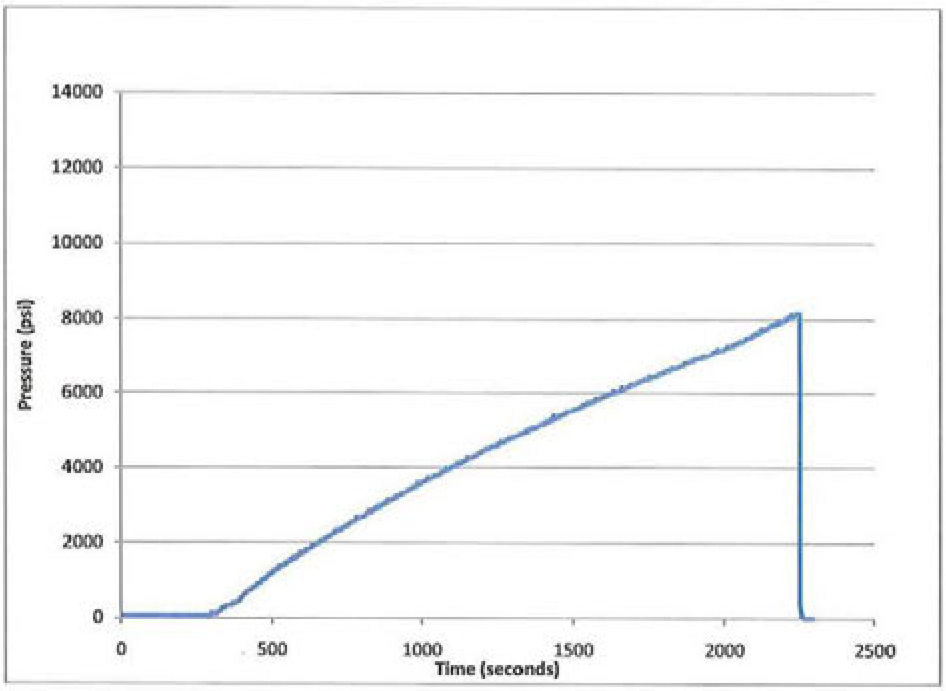

Figure B13: Pressure vs. Time - Tank 3B, 40% Flaw, No Cycles

APPENDIX C

Cylinder carcass after burst

Figure C1: Tank 5 Burst Carcass

Figure C2: Tank 5 Burst Carcass

Figure C3: Tank 4A Burst Carcass

Figure C4: Tank 4A Burst Carcass

Figure C5: Tank 1A Burst Carcass

Figure C6: Tank 1A Burst Carcass

Figure C7: Tank 2A Burst Carcass

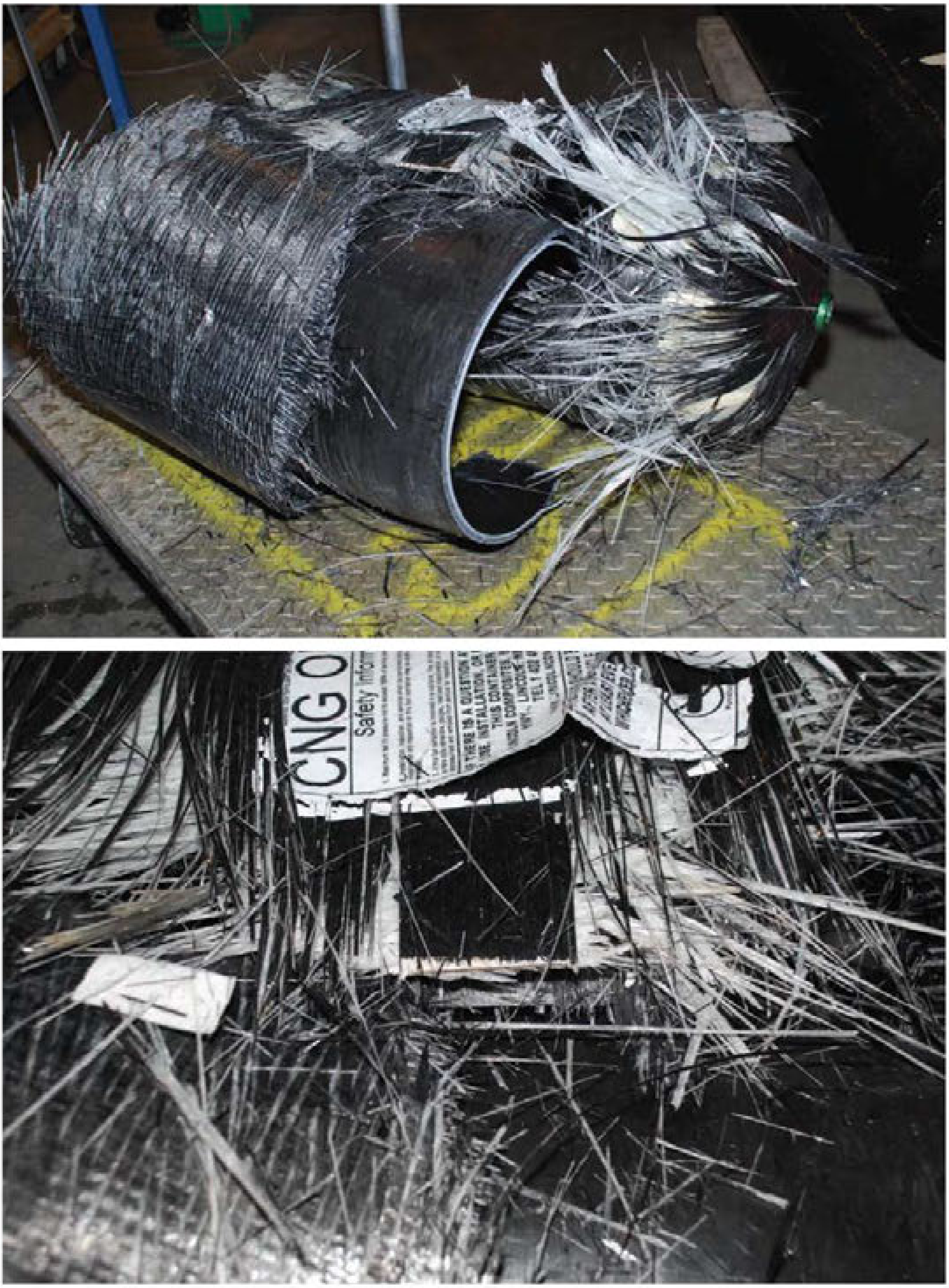

Figure C8: Tank 2A Burst Carcass

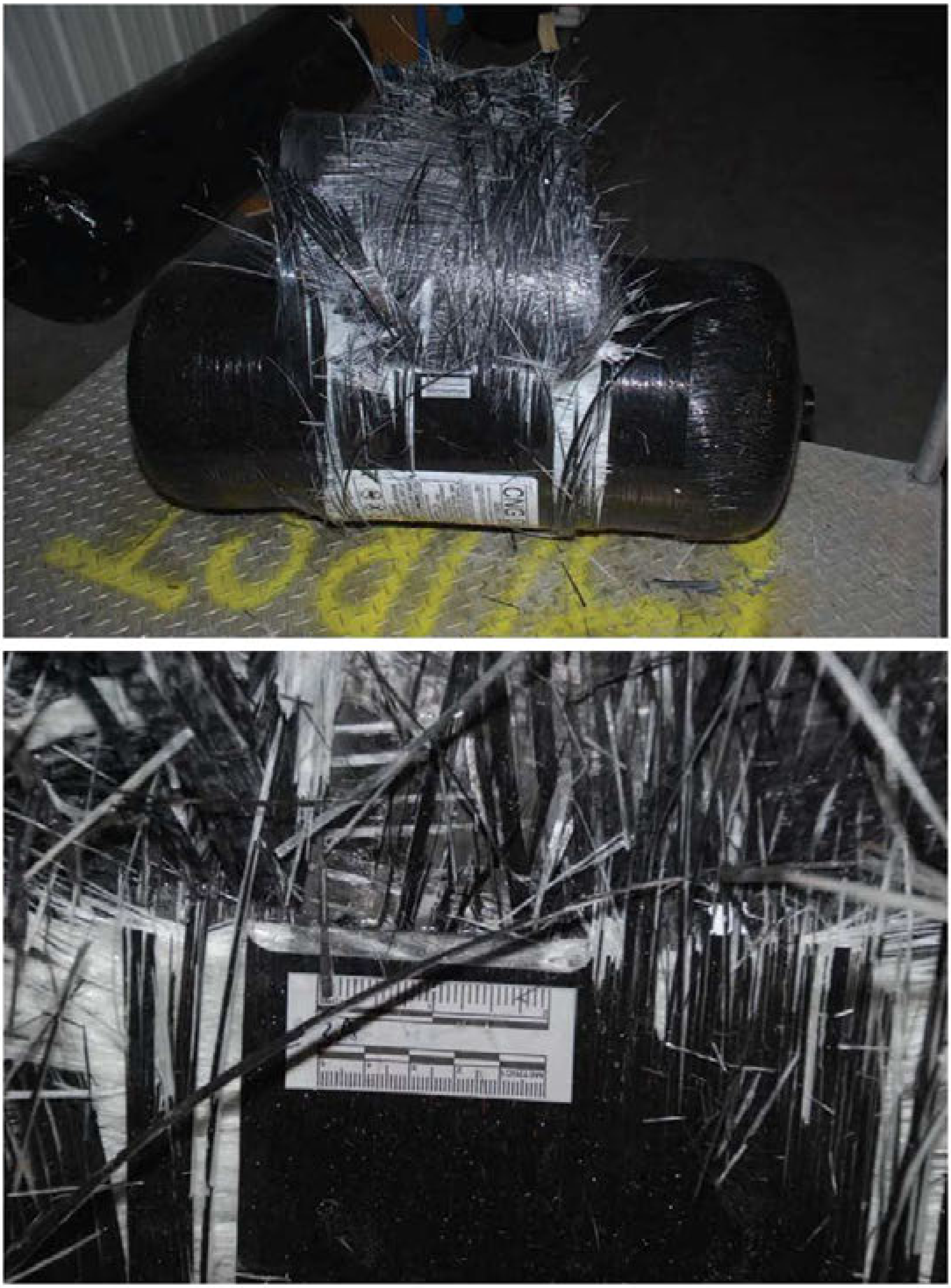

Figure C9: Tank 3A Burst Carcass

Figure C10: Tank 3A Burst Carcass

Figure C11: Tank 4C Burst Carcass

Figure C12: Tank 4C Burst Carcass

Figure C13: Tank 1C Burst Carcass

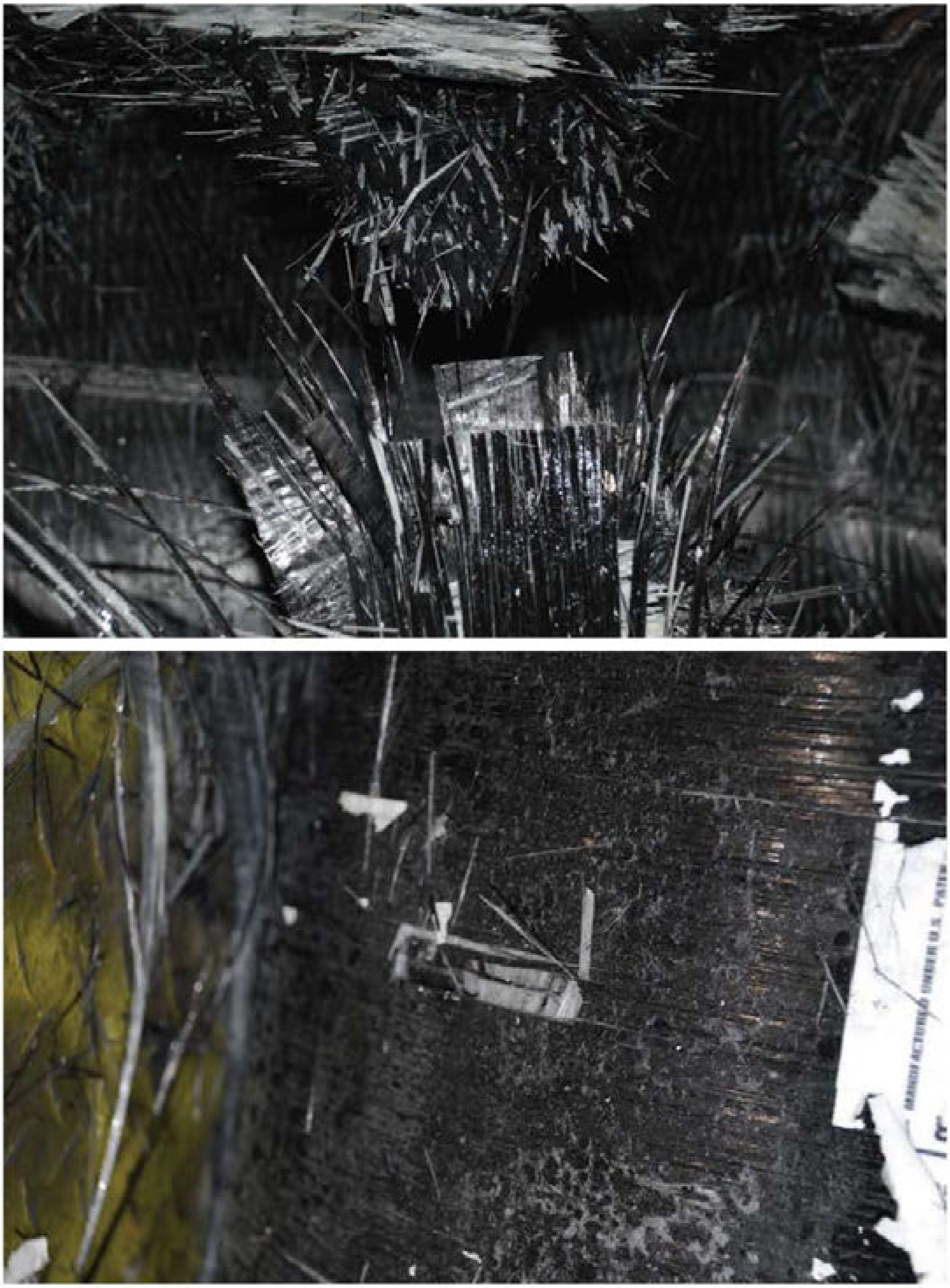

Figure C14: Tank 1C Burst Carcass

Figure C15: Tank 2C Burst Carcass

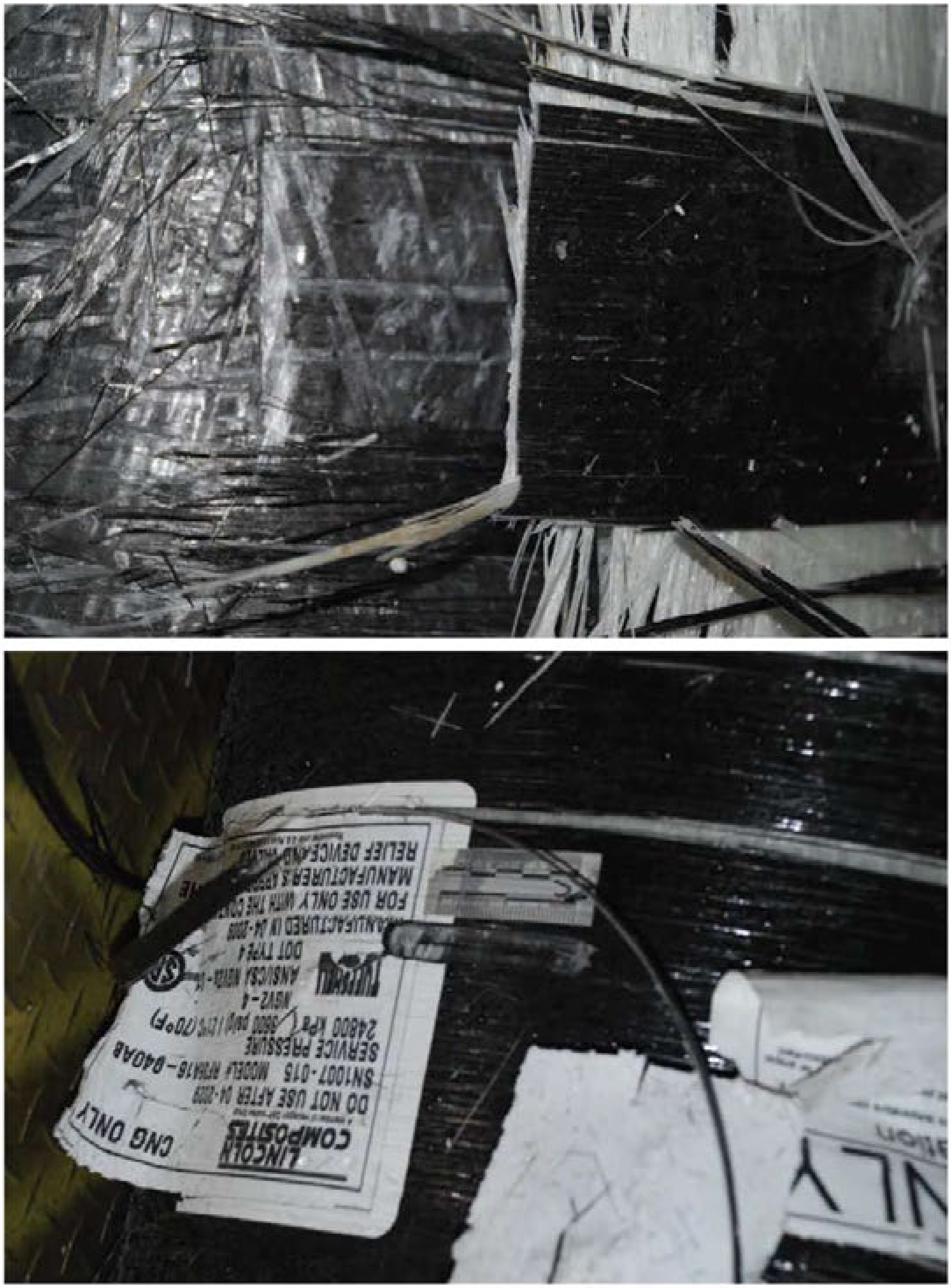

Figure C16: Tank 2C Burst Carcass

Figure C17: Tank 3C Burst Carcass

Figure C18: Tank 3C Burst Carcass

Figure C19: Tank 4B Burst Carcass

Figure C20: Tank 4B Burst Carcass

Figure C21: Tank 1B Burst Carcass

Figure C22: Tank 1B Burst Carcass

Figure C23: Tank 2B Burst Carcass

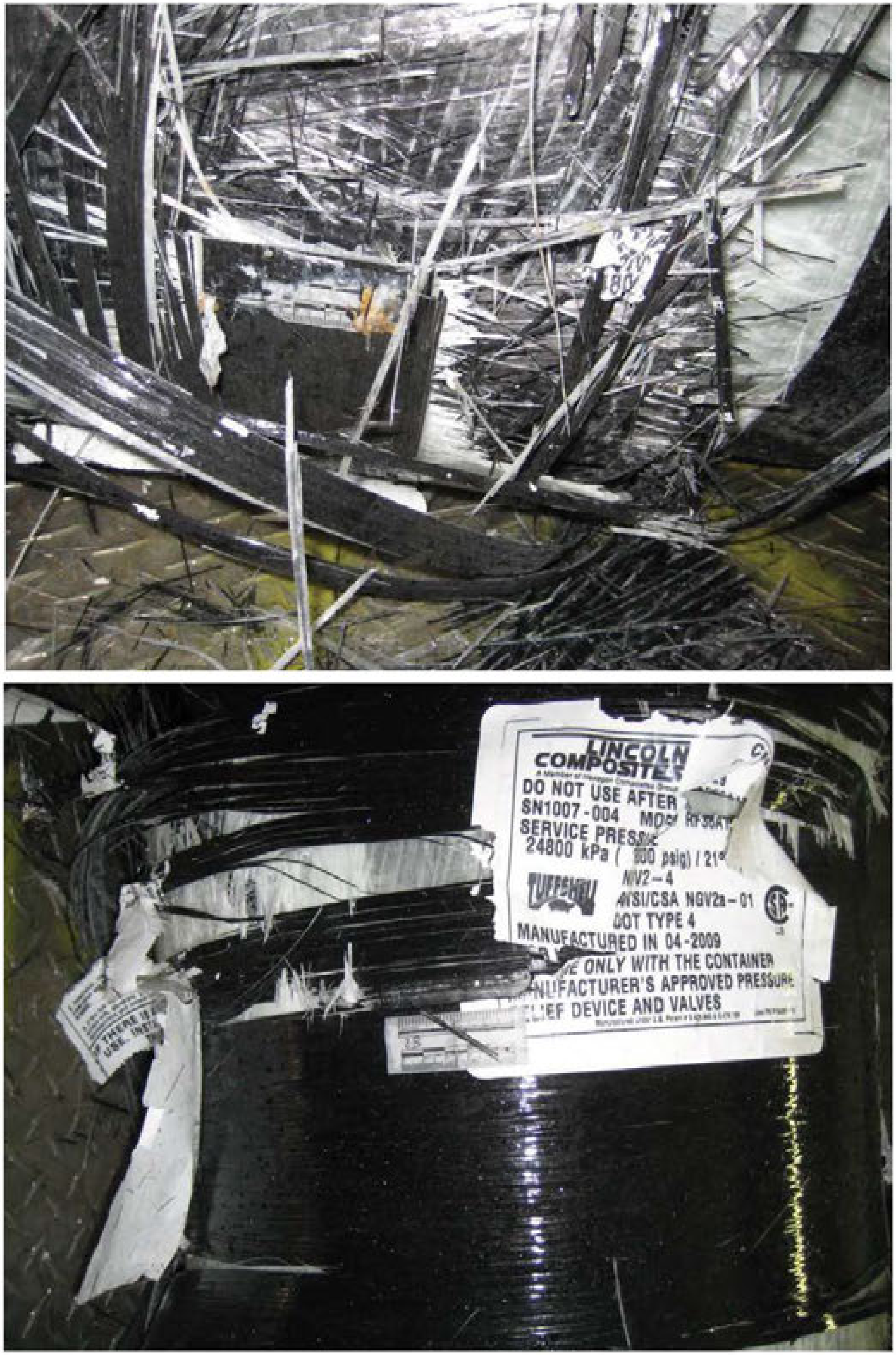

Figure C24: Tank 2B Burst Carcass

Figure C25: Tank 3B Burst Carcass

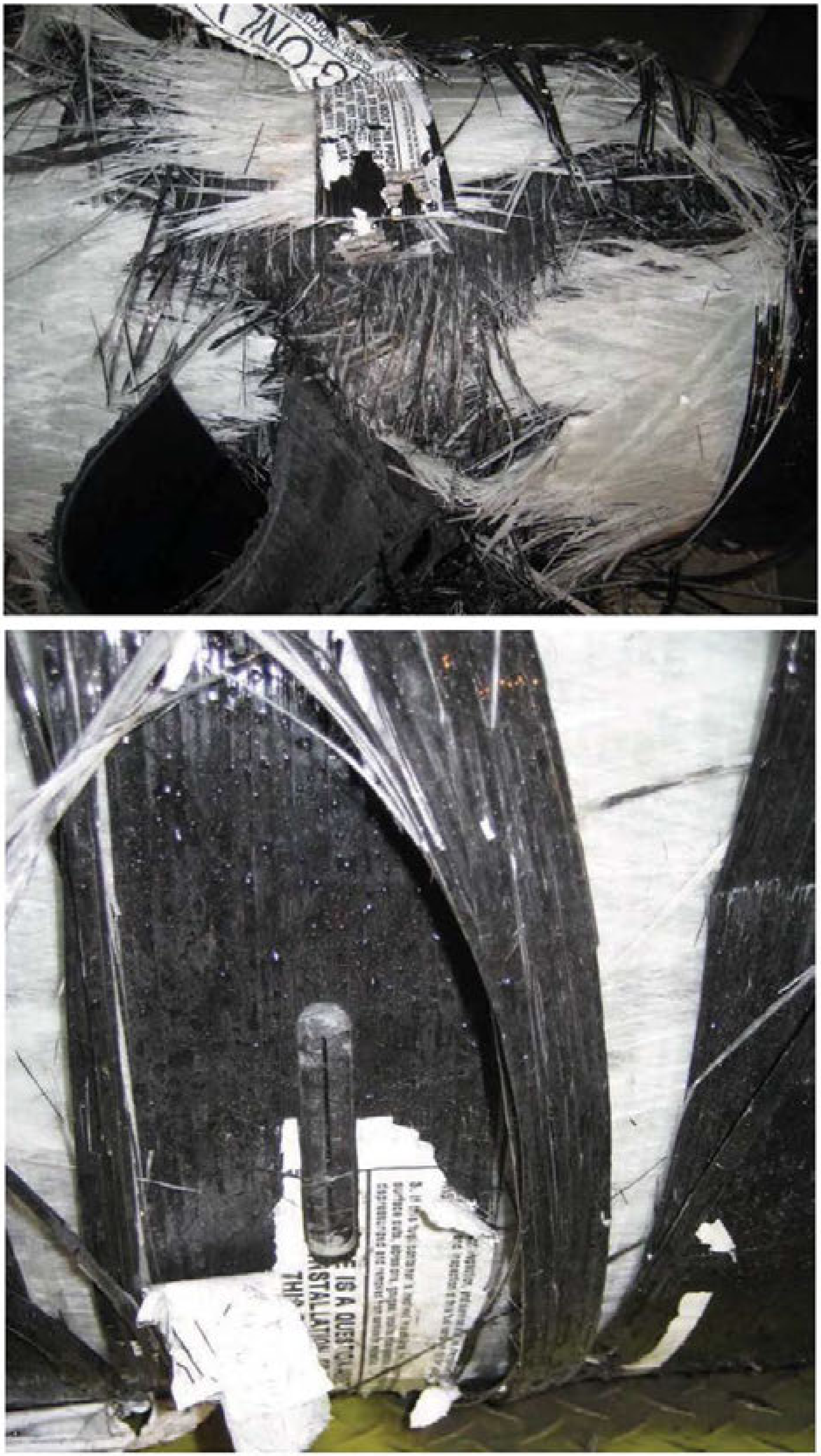

Figure C26: Tank 3B Burst Carcass

ACKNOWLEDGMENTS

This report was prepared by Lincoln Composites, Inc. The authors acknowledge, with deep appreciation, the activities of ASME ST-LLC and ASME staff and volunteers who have provided valuable technical input, advice and assistance with review and editing of, and commenting on, this document.

ISBN 978-0-7918-3353-7

9 780791 833537

A20911